ITERATIVE CHANNEL ESTIMATION TECHNIQUES FOR MULTIPLE INPUT MULTIPLE OUTPUT ORTHOGONAL FREQUENCY DIVISION MULTIPLEXING SYSTEMS

A Thesis Submitted to
the Graduate School of Engineering and Sciences of
İzmir Institute of Technology
in Partial Fulfillment of the Requirements for the Degree of

MASTER OF SCIENCE

in Electrical and Electronics Engineering

by
İlhan BAŞTÜRK

July 2007
İZMİR

We approve the thesis of **İlhan BAŞTÜRK**

Date of Signature

. . . . . **19 July 2007**
Assist. Prof. Dr. Berna ÖZBEK
Supervisor
Department of Electrical and Electronics Engineering
İzmir Institute of Technology

. . . . . **19 July 2007**
Assist. Prof. Dr. Mustafa Aziz ALTINKAYA
Department of Electrical and Electronics Engineering
İzmir Institute of Technology

. . . . . **19 July 2007**
Assist. Prof. Dr. Radosveta SOKULLU
Department of Electrical and Electronics Engineering
Ege University

. . . . . **19 July 2007**

Prof. Dr. F.Acar SAVACI
Head of Department
Department of Electrical and Electronics Engineering
İzmir Institute of Technology

. . . . . .
Prof. Dr. M. Barış ÖZERDEM
Head of the Graduate School

ACKNOWLEDGEMENTS

I would like to express my sincere gratitude to my advisor Asst. Prof. Dr. Berna Özbek for her valuable guidance and support. I am very proud that I had the chance to work with her.

I would like to thank to the members of my Thesis Committee Asst. Prof. Dr. Radosveta Sokullu and Asst. Prof. Dr. Mustafa Altınkaya for their useful comments.

I am deeply thankful to my parents Ahmet and Sabriye, and my brothers Mustafa and Hayati for their support and endless love through my life. Finally, I would like to thank my nieces Meliha and Burcu for making the hard times easier for me, with their joy and fun.

ABSTRACT

ITERATIVE CHANNEL ESTIMATION TECHNIQUES FOR MULTIPLE INPUT MULTIPLE OUTPUT ORTHOGONAL FREQUENCY DIVISION MULTIPLEXING SYSTEMS

Orthogonal frequency division multiplexing (OFDM) is well-known for its efficient high speed transmission and robustness to frequency-selective fading channels. On the other hand, multiple-input multiple-output (MIMO) antenna systems have the ability to increase capacity and reliability of a wireless communication system compared to single-input single-output (SISO) systems. Hence, the integration of the two technologies has the potential to meet the ever growing demands of future communication systems. In these systems, channel estimation is very crucial to demodulate the data coherently. For a good channel estimation, spectral efficiency and lower computational complexity are two important points to be considered. In this thesis, we explore different channel estimation techniques in order to improve estimation performance by increasing the bandwidth efficiency and reducing the computational complexity for both SISO-OFDM and MIMO-OFDM systems. We first investigate pilot and Expectation-Maximization (EM)-based channel estimation techniques and compare their performances. Next, we explore different pilot arrangements by reducing the number of pilot symbols in one OFDM frame to improve bandwidth efficiency. We obtain the bit error rate and the channel estimation performance for these pilot arrangements. Then, in order to decrase the computational complexity, we propose an iterative channel estimation technique, which establishes a link between the decision block and channel estimation block using virtual subcarriers. We compare this proposed technique with EM-based channel estimation in terms of performance and complexity. These channel estimation techniques are also applied to STBC-OFDM and V-BLAST structured MIMO-OFDM systems. Finally, we investigate a joint EM-based channel estimation and signal detection technique for V-BLAST OFDM system.

ÖZET

ÇOK-GİRİŞLİ ÇOK-ÇIKIŞLI DİK FREKANS BÖLMELİ ÇOĞULLAMA SİSTEMLERİ İÇİN DÖNGÜLÜ KANAL KESTİRİM TEKNİKLERİ

Dik frekans bölmeli çoğullama (DFBÇ), yüksek iletişim hızı ve frekans seçici kanallara karşı dayanıklılığı nedeniyle tercih edilen bir yöntemdir. Diğer taraftan, çok-girişli çok-çıkışlı (ÇGÇG) anten sistemleri, tek-girişli tek-çıkışlı (TGTÇ) kablosuz haberleşme sistemleriyle karşılaştırıldığında kapasiteyi ve güvenilirliği arttırma yeteneğine sahiptir. Dolayısıyla, bu iki teknolojinin birleşmesi ile gelecek haberleşme sistemlerinin yüksek veri hızı ve kapasite gibi ihtiyaçları karşılanacaktır. Bu sistemlerde gönderilen verinin düzgün geri alınabilmesi için iyi bir kanal kestirimine ihtiyaç duyulmaktadır. Bant genişliğinin verimli kullanılması ve hesaplama karmaşıklığının düşürülmesi iyi bir kanal kestirimi için göz önünde bulundurulması gereken iki önemli kıstastır. Bu tezde, biz TGTÇ-DFBÇ sistemler ve ÇGÇG-DFBÇ sistemlerde performansı arttırmak için bant genişliğini hesaplı kullanan, karmaşıklığı az değişik kanal kestirim algoritmalarını araştırdık. İlk olarak, pilot semboller ve Beklenti En Büyükleme algoritması ile kanal kestirimi teknikleri üzerine çalıştık ve bunları performans açısından karşılaştırdık. Daha sonra bant genişliğini verimli kullanmak için bir DFBÇ çerçevesinde kullanılan pilot sembol sayısını düşürerek farklı pilot yerleşimlerini karşılaştırdık. Bu pilot yerleşimlerine ait bit hata oranı ve kanal kestirimi başarım sonuçlarını elde ettik. Sonraki aşamada DFBÇ sistem modelinde karar verme bloğu ve kanal kestirim bloğu arasında bağlantı kuran döngülü kanal kestirim tekniğini önerdik ve bu önerdiğimiz tekniği performans ve hesaplama karmaşıklığı açısından Beklenti En Büyükleme algoritmasıyla karşılaştırdık. Bu kanal kestirim tekniklerini ayrıca uzay-zaman blok kodlu (UZBK)-DFBÇ ve V-BLAST yapılı ÇGÇG-DFBÇ sistemlere de uyguladık. Son olarak V-BLAST yapılı ÇGÇG-DFBÇ sistemler için kanal kestirimini ve sinyal sezimini birleşik olarak gerçekleştirdik ve kestirilen kanal katsayılarını Beklenti En Büyükleme algoritması kullanarak düzeltmeye çalıştık.

TABLE OF CONTENTS

LIST OF FIGURES

Figure **Page**

LIST OF TABLES

LIST OF ABBREVIATIONS

AWGN	Additive white Gaussian Noise
BLAST	Bell Labs layered space-time
BER	Bit error rate
CIR	Channel impulse response
CP	Cyclic prefix
CRLB	Cramer-Rao lower bound
CSI	Channel state information
D-BLAST	Diagonal BLAST
DAB	Digital audio broadcasting
DFT	Discrete fourier transform
DVB-T	Digital video broadcasting-terresterial
EM	Expectation-maximization
FFT	Fast Fourier transform
iid	Independent and identically distributed
ICI	Intercarrier interference
IFFT	Inverse Fast Fourier transform
ISI	Intersymbol interference
LAN	Local area network
LOS	Line-of-sight
LS	Least square
MAN	Metropolitan area network
MIMO	Multiple-input multiple-output
ML	Maximum-likelihood
MMSE	Minimum mean squared error
MSE	Mean squared error
OFDM	Orthogonal frequency division multiplexing
PDP	Power delay profile
PSK	Phase shift keying
QAM	Qadrature amplitude modulation

rms	Root mean squared
SISO	Single-input single-output
SM	Spatial multiplexing
SNR	Signal-to-noise ratio
STBC	Space-time block code
STC	Space-time code
STTC	Space-time Trellis code
SVD	Singular value decomposition
V-BLAST	Vertical BLAST
ZF	Zero forcing

CHAPTER 1

INTRODUCTION

1.1. Overview

High data rates are required for the future wireless communication systems to deliver multimedia services such as data, voice, image etc. However, the limited bandwidth and wireless channel impairments such as multipath propagation put some limitations to these systems. Multipath is the result of reflection of wireless signals by objects in the environment between the transmitter and receiver. Thus, the transmitted signal arrives at the receiver through multiple paths, with different attenuations, time delays and phases and this causes deep fades in signal strength. One way to effectively combat the multipath channel impairments and still provide high-data rates in a limited bandwidth is use of an orthogonal frequency-division multiplexing (OFDM) modulation method (Cimini 1985). OFDM is a special case of multi-carrier modulation technique. It is very attractive because of its high spectral efficiency and simple one-tap equalizer structure, as it splits the entire bandwidth into a number of overlapping narrow band subchannels requiring lower symbol rates. Furthermore, the inter-symbol interference (ISI) and intercarrier interference (ICI) can be easily eliminated by inserting a cyclic prefix (CP) to each transmitted OFDM symbol.

Multiple-input multiple-output (MIMO) systems adopt multi antenna arrays either on the transmitter side or receiver side. The MIMO techniques can be implemented to obtain a capacity gain in rich scattering environments without increasing the bandwidth or transmit power and to obtain the diversity gain to combat signal fading. Thus, these systems gained considerable interest in recent years. Many researchers explored the Space-Time Coding (STC) techniques and Spatial Multiplexing (SM) techniques to achieve capacity and diversity gain. The two forms of STC, Space-Time Trellis Code (STTC) is given in (Tarokh et al. 1998) and Space-Time Block Code is given in (Alamouti 1998). SM techniques as vertical BLAST (Bell Laboratories Layered Space Time) is given in (Wolniansky et al. 1998) and diagonal BLAST is given in (Foschini 1996). In layered systems, the input data stream is demultiplexed, independently encoded using

one-dimensional coding, and sent via different transmit antennas simultaneously. The received signal from each substream is separated by nulling according to zero-forcing (ZF) or minimum mean square-error (MMSE) criterion and successive interference cancellation (SIC).

The STC and BLAST systems are generally designed for flat fading channel types. However, many communication channels are frequency-selective fading in nature. A simple solution for this situation is to use OFDM, which converts frequency-selective fading channel into many narrow flat fading channels. Thus, the combination of MIMO and OFDM is a strong candidate for the future wireless communication systems. The MIMO systems combined with OFDM in the time domain are using space-time trellis coded (STTC)-OFDM (Agrawal et al. 1998, Lu and Wang 2000) or space-time block coded (STBC)-OFDM systems (Lee and Williams 2000).

These communication systems require a good channel estimate to demodulate the transmitted data coherently. Thus, channel estimation for single-input single-output (SISO)-OFDM and MIMO-OFDM systems has become a good research area in recent years. For SISO-OFDM systems, pilot-symbol aided channel estimation (Coleri et al. 2002) and blind channel estimation are two main channel estimation techniques used in the literature. Pilot-aided channel estimation technique is more reliable, less complex but spectrally inefficient. In order to estimate the channel coefficients for pilot-aided technique, estimation algorithms such as Least Squares (LS) or Minimum Mean Squared Error (MMSE) (Van de Beek et al. 1995) and interpolation techniques are used in time and frequency axes. Many different algorithms are also studied in order to improve the channel estimation performance in the literature. Expectation-Maximization (EM) algorithm (Dempster et al. 1977), which is a technique for finding the maximum-likelihood estimates of system parameters in the presence of unobserved data, is one of these algorithms. It is used for OFDM systems in (Ma et al. 2004). For MIMO-OFDM systems these techniques are also applied to estimating the channel (Barhumi et al. 2003). However, channel estimation for MIMO-OFDM systems is not as easy as for SISO-OFDM systems. In a MIMO system, multiple channels have to be estimated simultaneously. The increased number of channel unknowns significantly increases the computational complexity of the channel estimation algorithm.

In this thesis, we focus on different channel estimation techniques to improve the

estimation accuracy by using the bandwidth efficient techniques and reducing the computational complexity for SISO-OFDM and MIMO-OFDM systems. Firstly, we explore pilot based channel estimation and EM-based channel estimation techniques and study on different methods which have different pilot arrangements. Then, we propose a spectrally efficient channel estimation technique for SISO-OFDM systems with lower complexity and compare it to EM-based channel estimation. Then, we modify these estimation techniques and apply them to STBC-OFDM and V-BLAST structured MIMO-OFDM systems. Finally, we give the performance of these algorithms in terms of mean squared error (MSE), bit error rate (BER) and complexity comparing iteration numbers for EM algorithm.

1.2. Thesis Outline

In chapter 2, background information on wireless communication channels is provided. Also, an introduction to OFDM and MIMO systems is given. Space-Time coding and Spatial mutiplexing techniques are expressed in detail.

In chapter 3, an overview is given for OFDM channel estimation. Then, channel estimation techniques such as pilot-based and EM-based are defined and the performance results are compared. After that, two different methods with different number of pilots and pilot arrangement structure are designed and the performance results are compared (Baştürk and Özbek 2007). Finally, an iterative channel estimation technique with virtual subcarriers is proposed and the performance results are compared to EM-based channel estimation.

In chapter 4, MIMO-OFDM systems are examined in detail, including Space-Time Block Codes (STBC) and Vertical BLAST (V-BLAST) OFDM system models. Then, channel estimation techniques are explained for MIMO-OFDM systems and simulation results belonging to STBC-OFDM and V-BLAST structured OFDM channel estimation are given.

In chapter 5, a conclusion of the work directions presented in this thesis is given and some possible future works are suggested to extend this research.

CHAPTER 2

BACKGROUND

This chapter provides background on some of the fundamental concepts. The characteristics of the wireless communication channel are described in section 2.1, followed by an overview of OFDM in section 2.2. Finally, the background on MIMO systems are described in section 2.3.

2.1. Wireless Channel Characteristics

The characteristics of the wireless communication channel between transmitter and receiver controls the performance of the overall system. Thus, in order to model a wireless communication system we first need to understand the wireless characteristics so that a correct channel model can be developed. In this section, the mobile radio environment which will be used in this thesis is introduced.

There are two types of fading effects called as large-scale fading and small-scale fading that characterize mobile communications (Rappaport 1996). Large-scale fading represents the average signal power attenuation or path-loss due to the motion over large areas. In this type of fading the receiver is shadowed by obstacles between the tranmitter-receiver pair. Small-scale fading is used to describe the rapid fluctuations of the amplitude of a radio signal over a short period of time or travel distance. Multipath propagation and Doppler shift are the physical factors influencing small-scale fading. The transmitted signal could arrive at the receiver through multiple paths, with different attenuations, time delays and phases and this is called multipath. This effect results in constructive or destructive summation of the transmitted signal and causes a significant attenuation to the signal strenght. Furthermore, a relative motion between the transmitter and receiver also causes significant attenuations of the signal power within a short period of time which is called Doppler shift. With all these impairments, it is very challenging to overcome this time varying nature of the multipath wireless channel.

In this thesis, small-scale fading effect will be examined and large-scale fading effect of the channel will not be considered. Next, we will describe the multipath fading

effect in detail.

2.1.1. Multipath Fading Channel Model

Multipath fading effect occurs in almost all environments in wireless communications. In built up urban areas, fading occurs because the height of the mobile antennas are lower than the height of surrounding structures, so there is no single line-of-sight (LOS) path to the receiver. Thus, as shown in Figure 2.1, the transmitted signal arrives at the receiver through many different paths due to reflection, refraction or diffraction over large objects. Hence a reliable channel model must be defined to study on wireless communication system.

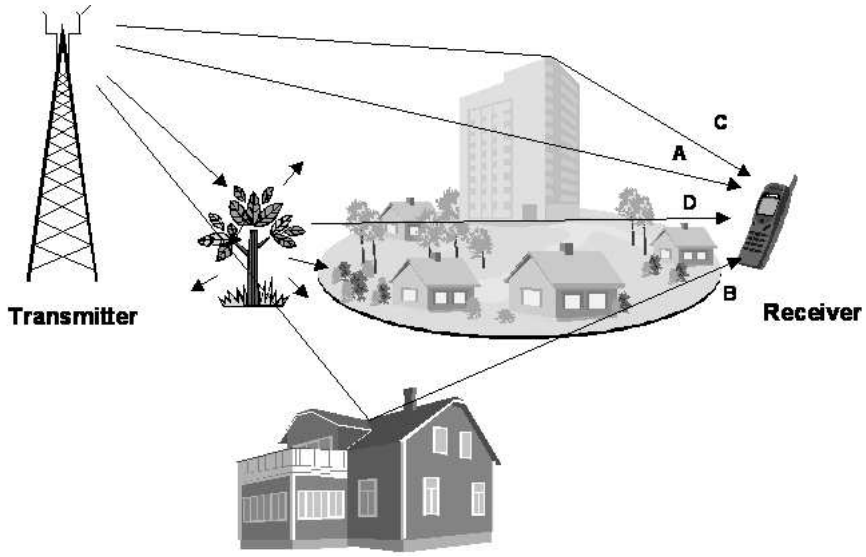

Figure 2.1. Multipath Propagation

Multipath fading channels have been modelled and simulated for the first time in the 1950s and early 1960s (Bello 1963, Clarke 1968, Jakes 1974). According to these channel models the multipath channel is a summation of the transmitted signal replicas with different amplitudes, propagation delays, phases and angles of arrival.

The impulse response of the mobile channel is very important while modelling the multipath channel. It is a wideband characterization and contains all information necessary to simulate or analyze any type of radio transmission through the channel. It can also be used to predict or compare the performance of many different mobile communication systems. The channel impulse response (CIR) of the multipath channel is modelled as,

$$h(t,\tau) = \sum_{l=0}^{L-1} \alpha_l(t) e^{j\theta_l(t)} \delta(\tau - \tau_l(t)) \tag{2.1}$$

where $\alpha_l(t)$ is the real amplitude and $\theta_l(t)$ is the phase value of the lth multipath component at time t, τ_l is the excess time that belongs to lth path. L is the total number of multipath components and δ is the unit impulse function that determines the specific excess delay of a multipath at time t.

If the channel impulse response is assumed to be constant over the transmission, it is simplified as follows,

$$h(\tau) = \sum_{l=0}^{L-1} \alpha_l e^{-j\theta_l} \delta(\tau - \tau_l). \tag{2.2}$$

The amplitudes of paths, which arrive at the receiver at the same time delay with different phases, could add constructively or destructively. Also, within a short period of time the phases of these paths may change. Thus, the resulting amplitude of the channel at a particular time delay could vary within a short time interval. When there are many paths, having independent amplitudes and phases, the channel impulse response $h(t,\tau)$ can be modelled as a complex Gaussian random process based on the central limit theorem. Furthermore, if there is no LOS component from the transmitter to the receiver, the amplitude of the channel can be modelled as Rayleigh fading channel. However, if there is a dominant LOS component, it can be modelled as Ricean fading channel. In this thesis, we will focus on Rayleigh fading channels.

The power and delay of each path can be determined by the power-delay profile (PDP) which is generally represented as plots of relative received power as a function of delay spread with respect to time. There are several parameters, which also can be derived from PDP, used for characterizing the wireless channel. Mean excess delay is a time dispersion parameter given as:

$$\bar{\tau_d} = \frac{\sum_{l=1}^{L} P(\tau_l)\tau_l}{\sum_{l=1}^{L} P(\tau_l)} \tag{2.3}$$

where $P(\tau_l)$ is the power of the lth path and τ_l is the arrival time of the lth path and also named the delay of the lth path. The root mean squared (rms) delay spread is a second time dispersion parameter, given as:

$$\sigma_{\tau_d} = \sqrt{\bar{\tau_d^2} - (\bar{\tau_d})^2} \tag{2.4}$$

where

$$\bar{\tau_d^2} = \frac{\sum_{l=1}^{L} P(\tau_l)\tau_l^2}{\sum_{l=1}^{L} P(\tau_l)}. \tag{2.5}$$

Typical values of the rms delay spread are on the order of microseconds in outdoor mobile radio channels and on the order of nanoseconds in indoor radio channels (Rappaport 1996).

While the delay spread is a natural phenomenon caused by reflected and scattered propagation paths in the radio channel, the coherence bandwidth is a defined relation derived from the rms delay spread. Coherence bandwidth is a statistical measure of the range of frequencies over which the channel can be considered flat. In other words, coherence bandwidth is the range of frequencies over which two frequency components have a strong potential for amplitude correlation. Two sinusoids with frequemcy seperation greater than B_c are affected quite differently by the channel. If the coherence bandwidth is defined as the bandwidth over which the frequency correlation function is above 0.9, then the coherence bandwidth can be defined in terms of rms delay spread as (Rappaport 1996) :

$$B_c = \frac{1}{50\sigma_{\tau_d}}. \tag{2.6}$$

A more relaxed definition where the frequency correlation function is above 0.5 yields approximately as:

$$B_c = \frac{1}{5\sigma_{\tau_d}}. \tag{2.7}$$

Using the coherence bandwidth parameters multipath channel can be categorized into flat or frequency selective fading channels.

The parameters expressed above do not contain any information about the time varying nature of the channel caused by either relative motion between the transmitter and the receiver, or by the moving obstacles in the channel. Doppler spread and coherence time are parameters for describing the time varying nature of the channel. The spectral broadening caused by the time rate of change of the mobile radio channel is measured

by Doppler spread. As a time domain dual of the Doppler spread, coherence time is a statistical measure of the time duration over which the channel impulse response is invariant . These two parameters are inversely proportional to each other. If the coherence time is defined as the time over which the time correlation function is above 0.5, then the coherence time is

$$T_c = \frac{9}{16\pi f_d} \tag{2.8}$$

where $f_d = (v/c)f_c$ is the Doppler spread or Doppler frequency, v is the velocity of the mobile, f_c is the carrier frequency and c is the speed of the light.

Multipath fading channels can be categorized into fast or slow fading using coherence time parameters. The channel is called slow fading, if $T_s < T_c$ where T_s is symbol period and T_c is the coherence time. This type of channel has low Doppler spread and the impulse response of the channel changes at a rate much slower than the transmitted signal. When $T_s > T_c$, then the channel is said to be fast fading. This type of channel has high Doppler spread and the channel impulse response of the channel changes rapidly within the symbol duration.

In the following section flat fading and frequency-selective fading channels, which are expressed before, will be defined in detail.

2.1.1.1. Flat Fading Channel

A channel is called flat fading when the transmitted symbol duration is much larger than the time dispersion of the channel ($T_s >> \tau_d$, where T_s is the symbol duration and τ_d is the maximum delay spread), such that the multipath can not be resolved to more than one symbol time. In the frequency domain, a flat fading channel has a constant amplitude and linear phase response over the transmitted signal bandwidth (where the condition $B_c >> B_s$ is satisfied, with B_s being the transmission bandwidth). The spectral characteristic of the transmitted signal is preserved at the receiver for this fading type. In a flat fading channel, the CIR can be written as:

$$h(t) = \alpha(t)e^{j\theta(t)} \tag{2.9}$$

where $\alpha(t)$ is Rayleigh distributed for the channel without LOS path, and is Ricean distributed when LOS path exists and $\theta(t)$ is uniformly distributed.

2.1.1.2. Frequency-Selective Fading Channel

When the transmitted signal bandwidth is greater than the coherence bandwidth of the channel ($B_c \ll B_s$), the spectral characteristics of the signal cannot be maintained. In this case, the channel applies different gains or attenuations to different frequency components of the transmitted signal, causing spectral distortion in the signal. This kind of channel is called frequency-selective fading channel. From the time domain perspective, the symbol period is shorter than the rms delay spread. The channel will spread the signal beyond the symbol period and induce intersymbol interference (ISI) onto the next transmitted symbol. Using proper pulse shaping and matched filter at the receiver, the frequency-selective fading channel can be modelled as a tapped delay line with filter lenght L_t as shown in Figure 2.2.

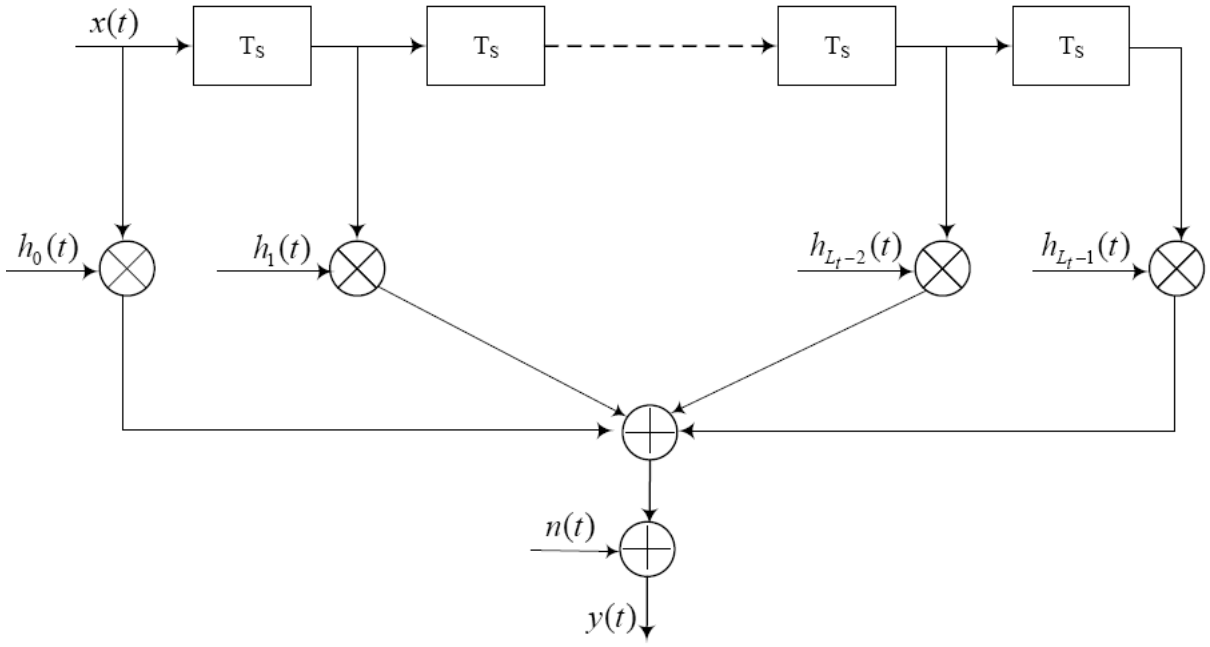

Figure 2.2. Tap delay line filter model for frequency-selective fading channels

Then the frequency-selective fading channels can be represented as:

$$h(t,\tau) = \sum_{l=0}^{L_t-1} h_l(t)\delta(\tau - lT_s) \tag{2.10}$$

where $h_l(t)$ is the complex path coefficient of the lth tap at time t whose amplitude is Rayleigh and phase is uniformly distributed, T_s is the symbol period. Frequency-selective

fading channels are much more difficult to model than flat-fading channels since each multipath signal must be modelled.

2.2. Orthogonal Frequency Division Multiplexing (OFDM)

The nature of wireless local area network (WLAN) applications demands high data rates. Naturally, dealing with unpredictable wireless channels at high data rates is not an easy task. Orthogonal frequency division multiplexing (OFDM) has received considerable interest in the last few years for its advantages in high data rate transmissions over frequency-selective fading channels. In OFDM, a wideband signal is split into multiple parallel narrowband signals, and then modulated onto orthogonal subcarriers for transmission (Cimini 1985). The OFDM transforms a frequency-selective fading channel into multiple parallel flat fading channels, which greatly simplifies the channel estimation and equalization tasks of the receiver. When a wideband signal passes through a frequency

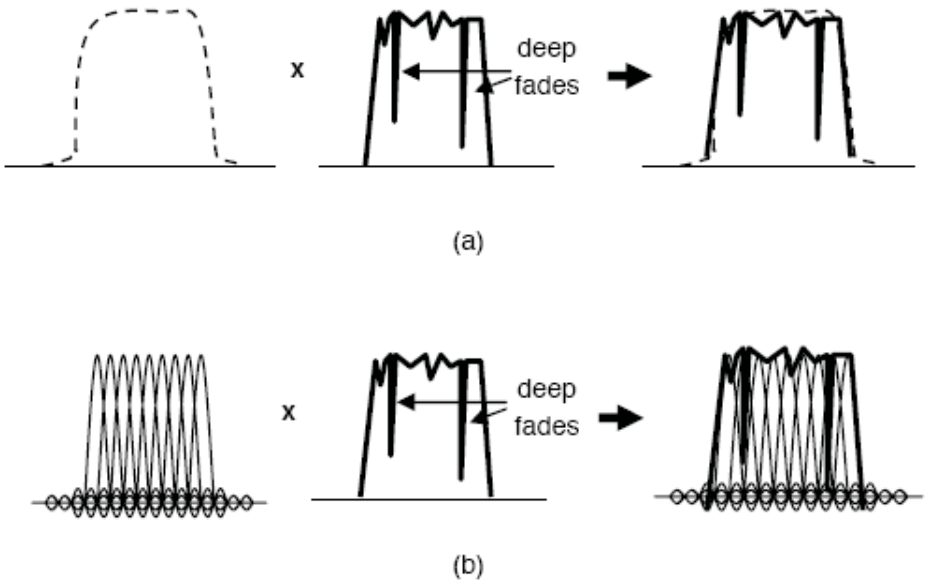

Figure 2.3. (a) A wideband channel multiplied with frequency selective fading channel. (b) An OFDM signal multiplied with frequency selective fading channel.

selective channel as shown in Figure 2.3 (a), a significant portion of the signal is lost due to the deep fades in the channel. However, when the wideband signal is OFDM modulated, the frequency spectrum will be a combination of overlapping narrowband signals as shown in Figure 2.3 (b). Now, when the OFDM modulated signal passes through the

frequency selective channel, only the narrowband signals at the location of the fades will be affected. OFDM also uses the available spectrum efficiently since the subcarriers are orthogonal to each other.

A schematic diagram of the complete structure of an OFDM system is shown in Figure 2.4. The input data stream is modulated using regular modulation techniques such as phase shift keying (PSK) or quadrature amplitude modulation (QAM). The modulated signal $X(k)$ ($k = 0, 1, ..., K-1$), where K is the number of the subcarriers, is passed through an Inverse Fast Fourier Transform (IFFT) block. The IFFT operation modulates the parallel signals onto orthogonal subcarriers as a group. The output symbols in the time domain are expressed as

$$x(m) = \frac{1}{\sqrt{K}} \sum_{k=0}^{K-1} X(k) e^{j2\pi mk/K}, \qquad 0 \leqslant m \leqslant K-1. \tag{2.11}$$

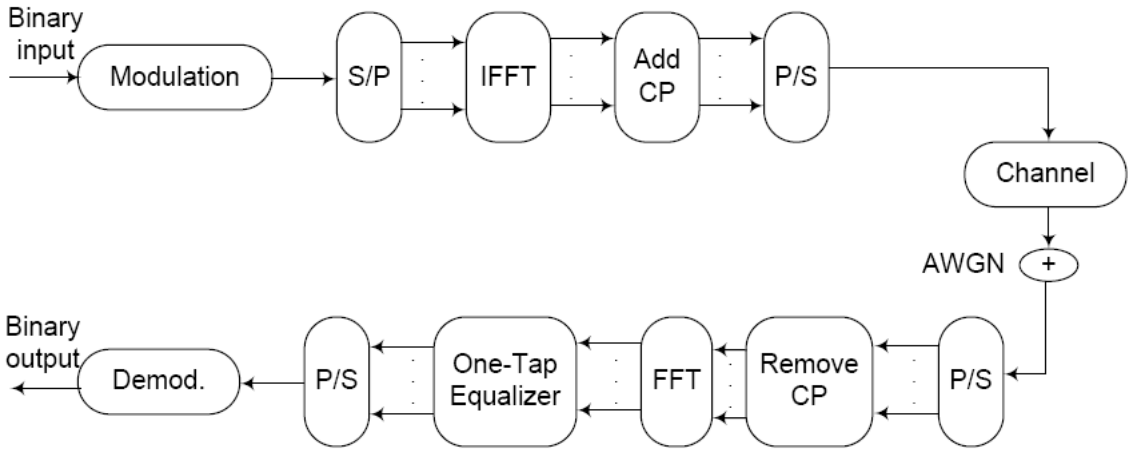

Figure 2.4. Basic OFDM Transceiver Structure

After the IFFT process, a cyclic prefix (CP) is added to the OFDM symbol in order to mitigate the ISI. The CP consists of copying the last part of the OFDM symbol and appending to front of the same OFDM symbol, $\tilde{x}[m] = \tilde{x}[-N_{cp}], ..., \tilde{x}[K-1] = x[K-N_{cp}], ..., x[0], ..., x[K-1]$ where N_{cp} is the lenght of CP. The CP helps to maintain orthogonality between the subcarriers because the orthogonality of the signal can be lost, when signal passes through a time-dispersive channel. Repeating the last elements at the beginning converts a linear convolution of the transmitted sequence and the channel

impulse response to a circular convolution. Thus, the channel estimation is performed simpler using one-tap equalizer at the receiver.

The OFDM signal with CP is then passed through the parallel-to-serial converter and send through the multipath channel. The transmitted signal is filtered by the channel impulse response $h(m)$ and corrupted by additive white Gaussian noise (AWGN), so the received signal is $y(m) = \tilde{x}[m] * h(m) + n(m), -N_{cp} \leqslant m \leqslant K-1$. The CP of $y(m)$ consisting of the first N_{cp} samples is then removed and the received signal is passed through a Fast Fourier Transform (FFT) block. So, the received signal in the frequency domain, $Y(k)$, is obtained as:

$$Y(k) = \frac{1}{\sqrt{K}} \sum_{m=0}^{K-1} y(m) e^{-j2\pi mk/K}, \qquad 0 \leqslant k \leqslant K-1. \tag{2.12}$$

It is mentioned above that the CP converts the linear convolution to the circular convolution. From the definition of the FFT, circular convolution in time leads to multiplication in frequency,

$$Y(k) = X(k)H(k) + N(k), \qquad 0 \leqslant k \leqslant K-1 \tag{2.13}$$

where $H(k)$ is the frequency response of the channel and $N(k)$ represents the AWGN component which has zero mean and σ_N^2 variance at subcarrier k. The FFT output is parallel-to-serial converted and then passed through the demodulator to recover the original data.

2.3. MIMO Systems

Multiple-Input Multiple-Output (MIMO) communication systems use multiple antennas at the transmitter and receiver to provide various gains. Two major gains over single-input single-output (SISO) systems in wireless channels are providing the high data rate without increasing the bandwidth or the transmission power and increasing the diversity to improve the performance against fading channels. Space time coding (STC) and spatial multiplexing (SM) techniques have been developed in order to exploit these benefits. SM techniques increase spectral efficiency and give strenght to communicate at high data rates by using layered space-time coding techniques and STC techniques improve the link reliability and overcome the different channel impairments.

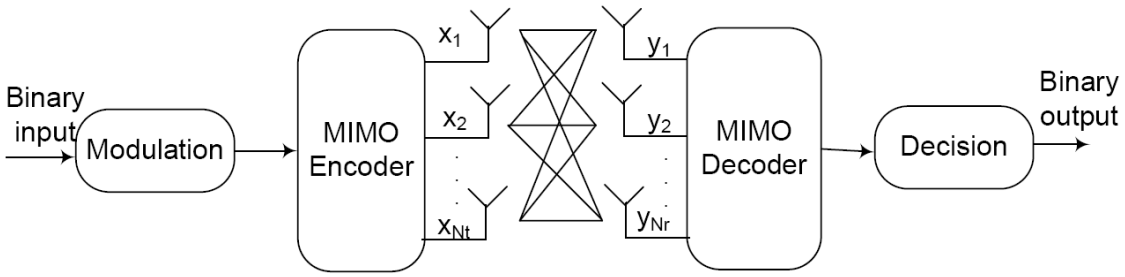

Figure 2.5. The MIMO wireless system

We can examine a MIMO wireless transmission system with N_t transmit antennas and N_r receive antennas illustrated in Figure 2.5. In this system, first of all the binary input data is modulated. Then, the modulated data is encoded with a MIMO encoder and transmitted from N_t transmit antennas.

For a flat-fading MIMO system with N_t transmit antennas and N_r receive antennas, the received signal at the jth receive antenna can be expressed as:

$$y_j = \sum_{i=1}^{N_t} x_i h_{ij} + n_j \tag{2.14}$$

where x_i is the symbol transmitted from the ith transmit antenna, h_{ij} is the complex channel coefficients from transmit antenna i to receive antenna j and n_j is the additive noise which is modelled as Gaussian that is assumed to be independent and identically distributed (i.i.d.) with zero mean and variance $\sigma_n^2 = N_0/2$. The transmitted signals from all transmit antennas overlap in time, space and frequency so that the received signal is a superposition of all transmitted signals distorted by the channel noise.

The channel coefficient matrix $\mathbf{H}$ with dimensions $N_r \times N_t$ is denoted as:

$$\mathbf{H} = \begin{bmatrix} h_{11} & \dots & h_{1N_t} \\ \vdots & \ddots & \vdots \\ h_{N_r1} & \dots & h_{N_rN_t} \end{bmatrix} \tag{2.15}$$

As a result, we can write the received signal given in Equation (2.14) in the matrix form as:

$$\mathbf{Y} = \mathbf{HX} + \mathbf{N} \tag{2.16}$$

where

$$\mathbf{Y} = \begin{bmatrix} y_1 \\ \vdots \\ y_{N_r} \end{bmatrix}, \ \mathbf{X} = \begin{bmatrix} x_1 \\ \vdots \\ x_{N_t} \end{bmatrix}, \ \mathbf{N} = \begin{bmatrix} n_1 \\ \vdots \\ n_{N_r} \end{bmatrix}. \tag{2.17}$$

As mentioned above, with channel knowledge at the receiver side only, we have two families of techniques to communicate over MIMO channels which are STC and SM.

2.3.1. Spatial Multiplexing (SM)

Spatial multiplexing also known as the Bell-labs LAyered Space Time (BLAST) system was first proposed by Foschini in (Foschini 1996). The goal of BLAST systems is to increase data rate in wireless radio link. There are two types of BLAST algorithms. These are known as the diagonal BLAST (D-BLAST) and the vertical BLAST (V-BLAST). The D-BLAST uses multiple antennas at both the transmitter and receiver, and a coding architecture that disperses the coded blocks across the diagonals in space-time. In a rich Rayleigh scattering environment, the capacity of this coding structure increases linearly with the number of antenna elements, up to 90% of the Shannon theoretical capacity limit. However, the complexities of D-BLAST implementation led to V-BLAST which is a modified version of BLAST (Wolniansky et al. 1998). The essential difference between D-BLAST and V-BLAST lies in their respective transmission coding processes. In D-BLAST, temporal redundancy is introduced between the substreams by dispersing the code blocks along the space-time diagonals. However, the encoding process is simply a demultiplexing operation in V-BLAST. An example with three antennas and hence three layers is shown in Figure 2.6(a). The three layers *a*, *b* and *c* are vertically stacked in the space-time grid, hence the name vertical BLAST. Since a layer is totally transmitted by a single antenna, this scheme cannot take advantage of the transmit diversity. The D-BLAST architecture is similar to the V-BLAST one except that each layer is spread over all the transmit antennas as it is illustrated in Figure 2.6(b). Each layer is diagonally placed in the space-time grid in this figure, hence the name diagonal BLAST. The first symbol of layer *a*, *a1*, is sent by the first antenna. The second symbol of this layer, *a2*, is sent by the second antenna, and so on. Since each layer is spread over all the transmit antennas, this scheme benefits from the transmit diversity. In this thesis, we will focus on V-BLAST algorithm.

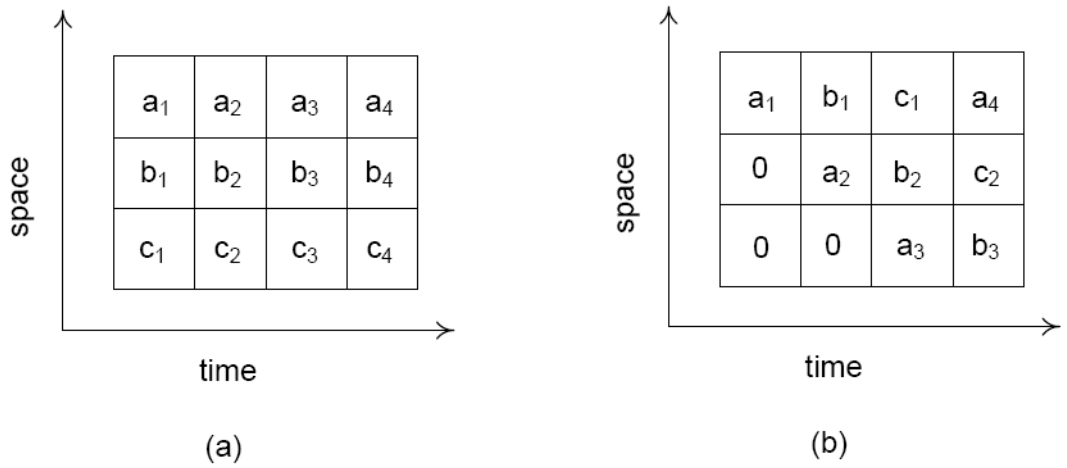

Figure 2.6. Space time grids for (a) V-BLAST (b) D-BLAST

2.3.1.1. V-BLAST

V-BLAST architecture was first proposed by Foschini in order to increase the capacity while exploiting multipath fading in (Wolniansky et al. 1998). Multiple transmit antennas are used to simultaneously transmit independent data, this results in an increase in the data rate proportional to the number of transmit antennas. Each transmitter uses the same frequency spectrum for every transmission which leads to high spectral efficiency.

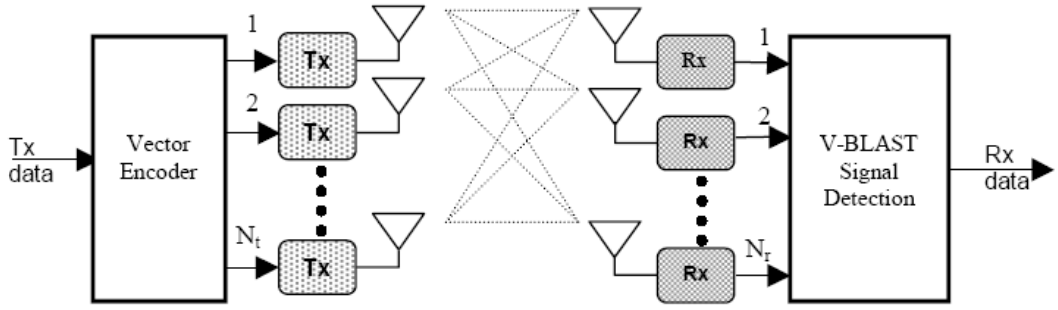

Figure 2.7. Block Diagram of the V-BLAST architecture

A block diagram of the V-BLAST architecture is given in Figure 2.7. There are N_t transmit antennas and N_r receive antennas, where $N_r \geqslant N_t$. The data is first demultiplexed into layers, and each layer is transmitted from a different antenna. Each antenna transmits the data layers simultaneously in the same frequency band. The channel is assumed to be quasi-static, flat, Rayleigh fading which is shown in matrix form with di-

mension $N_r \times N_t$ in Equation (2.15). The receivers operate co-channel where the signal at each receiver contains superimposed components of the transmitted signals. The received signal vector with size $N_r \times 1$ can be modelled as given in Equation (2.16).

The V-BLAST detection architecture employs a layered processing methodology, which includes inter-channel interference nulling, symbol detection and interference cancellation. The received signal from each substream is separated by nulling according to zero-forcing (ZF) or minimum mean square-error (MMSE) criterion and successive interference cancellation (SIC). An overview of ZF-SIC V-BLAST detection algorithm is as follows. At each symbol time, it first detects the strongest layer (transmitted signal), then cancels the effect of this strongest layer from each of the received signals, and then proceeds to detect the strongest of the remaining layers, and so on. By assuming the receiver perfectly knows the channel matrix $\mathbf{H}$, four recursive steps for ZF-SIC V-BLAST is given as:

Step 1. Ordering: Determine the optimal detection order which corresponds to choosing the row of $\mathbf{H}^{\dagger}$(pseudo inverse of $\mathbf{H}$) with minimum Euclidian norm.

$$\mathbf{G} = \mathbf{H}^{\dagger} = (\mathbf{H}^{*}\mathbf{H})^{-1}\mathbf{H}^{*} \tag{2.18}$$

$$k = \arg\min_{i} \|\underline{(\mathbf{G})_i}\|^2 \tag{2.19}$$

where $\mathbf{G}$ is referred to as nulling matrix, $\underline{(\mathbf{G})_i}$ is representing the ith row of the nulling matrix and $\mathbf{H}^{*}$ is the complex conjugate of the channel matrix $\mathbf{H}$.

Step 2. Nulling: Choose the row $\underline{(\mathbf{G})_k}$ as the nulling vector $\mathbf{w}_k$, use it to null out all the weaker transmit signals and obtain the strongest transmit signal y_k.

$$\mathbf{w}_k = \underline{(\mathbf{G})_k} \tag{2.20}$$

$$y_k = \mathbf{w}_k^{T}\mathbf{y} \tag{2.21}$$

where $\mathbf{y}$ is the total received signal vector which contains superimposed signals.

Step 3. Slicing: Detect the estimated value of the strongest transmit signal by slicing to the nearest value in the signal constellation Ω.

$$\hat{x}_k = \arg\min_{\hat{x}\epsilon\Omega} \|x - y_k\|^2 \tag{2.22}$$

Step 4. Cancellation: Once the strongest transmit signal has been detected, cancel its effect from the received signal vector in order to reduce the detection complexity for

remaining transmit signals.

$$\mathbf{y} \leftarrow \mathbf{y} - \hat{x}_k(\mathbf{H})_k \tag{2.23}$$

Correspondingly, the kth column $(\mathbf{H})_k$ of the channel matrix $\mathbf{H}$ should also be zeroed,

$$\mathbf{H} \leftarrow (\mathbf{H})_{\bar{k}} \tag{2.24}$$

The process described above corresponds to detecting one layer, after which we return to step 1 and detect the next layer.

V-BLAST systems can achieve the maximum mutual information which is equal to full multiple antenna channel capacity. Its drawbacks include its inability to work with fewer receive antennas than transmit antennas, and its absence of built-in spatial coding.

2.3.2. Space Time Coding (STC)

STC introduces redundancy in space, through the addition of multiple antennas, and redundancy in time, through channel coding. There are two main types of STCs, namely space-time block codes (STBC) (Alamouti 1998) and space-time trellis codes (STTC) (Tarokh et al. 1998). In contrast to single-antenna block codes for the AWGN channel, STBCs do not generally provide coding gain, unless concatenated with an outer code. Their main feature is to provide diversity gain, with very low decoding complexity. STTC provide both diversity and coding gain at the cost of higher decoding complexity.

2.3.2.1. Space Time Block Coding (STBC)

STBC technique was first proposed by Alamouti in (Alamouti 1998). The technique uses two transmit antennas to expand bandwidth or get diversity gain without introducing redundancy in the time or frequency domain. In this method, the input data stream is first mapped into symbols using a constellation mapper, and the symbol stream is then divided into two substreams. The symbols x_1 and x_2 are transmitted from the first and second antenna respectively at time t and the symbols $-x_2^*$ and x_1^* are transmitted from the first and second antenna respectively at time $t+T_s$. Alamouti's coding method at time and spatial domain is shown in Table 2.1.

In this case the code matrix can be given as:

$$\mathbf{X} = \begin{bmatrix} x_1 & x_2 \\ -x_2^* & x_1^* \end{bmatrix} \tag{2.25}$$

Table 2.1. Alamouti's coding method

	Antenna 1	Antenna 2
Time t	x_1	x_2
Time $t + T_s$	$-x_2^*$	x_1^*

The key feature of the Alamouti scheme is that the transmit sequences from the two transmit antennas are orthogonal since the code matrix has the following property $\mathbf{X}^H\mathbf{X} = (|x_1|^2 + |x_2|^2)\mathbf{I}_2$, where $\mathbf{I}_2$ is the 2×2 identity matrix.

Let's assume that one receiver antenna is used at the receiver. The block diagram of the Alamouti scheme is shown in Figure 2.8. The fading channel coefficients from the first and the second transmit antennas to the receive antenna at time t are denoted by $h_1(t)$ and $h_2(t)$, respectively. By assuming that the channel coefficients do not change in the interval from time t to $t + T_s$, they can be expressed as follows:

$$\begin{aligned} h_1(t) &= h_1(t + T_s) = h_1 = |h_1|e^{j\theta_1} \\ h_2(t) &= h_2(t + T_s) = h_2 = |h_2|e^{j\theta_2} \end{aligned} \tag{2.26}$$

where h_i and θ_i, $(i = 1, 2)$ are the amplitude gain and phase shift for the path from antenna i to the receive antenna and T_s is the symbol duration.

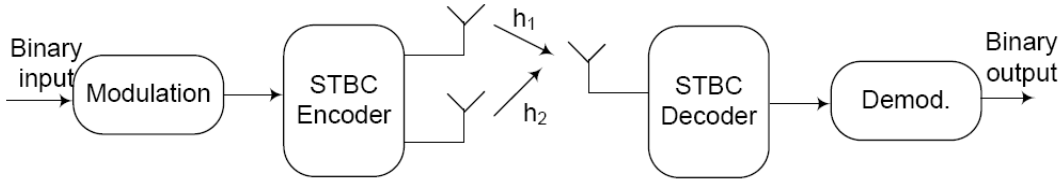

Figure 2.8. Alamouti STBC Block Diagram

The received signals at the receiver antenna over two consecutive symbol periods for time t and $t + T_s$ can be expressed as:

$$\begin{aligned} y_1 &= y(t) = x_1h_1 + x_2h_2 + n_1 \\ y_2 &= y(t + T_s) = -x_2^*h_1 + x_1^*h_2 + n_2 \end{aligned} \tag{2.27}$$

where n_1 and n_2 are additive white Gaussian noise with zero mean and power spectral density $N_0/2$. We can also write the Equation (2.27) in matrix form as:

$$\begin{bmatrix} y_1 \\ y_2 \end{bmatrix} = \begin{bmatrix} x_1 & x_2 \\ -x_2^* & x_1^* \end{bmatrix} \begin{bmatrix} h_1 \\ h_2 \end{bmatrix} + \begin{bmatrix} n_1 \\ n_2 \end{bmatrix} \tag{2.28}$$

When we take the complex conjugate of the received signal at time $t + T_s$, the received signal can be expressed as $\mathbf{Y} = [y_1 \ y_2^*]^T$. We can also write the transmitted signal as $\mathbf{X} = [x_1 \ x_2]^T$ and rewrite Equation (2.28) in a matrix/vector form as:

$$\mathbf{Y} = \mathbf{HX} + \mathbf{N} \tag{2.29}$$

where the channel matrix is given as:

$$\mathbf{H} = \begin{bmatrix} h_1 & h_2 \\ h_2^* & -h_1^* \end{bmatrix} \tag{2.30}$$

The transmitted signals can be decoded back by multiplying the received signal with the Hermitian of the $\mathbf{H}$ matrix $(\mathbf{H}^H)$ since the channel matrix $\mathbf{H}$ is orthogonal.

$$\tilde{\mathbf{X}} = \mathbf{H}^H \mathbf{Y} \tag{2.31}$$

Thus, we can find the decision statistics as

$$\begin{aligned} \tilde{x}_1 &= h_1^* y_1 + h_2 y_2^* \\ \tilde{x}_2 &= h_2^* y_1 - h_1 y_2^*. \end{aligned} \tag{2.32}$$

Substituting y_1 and y_2 from Equation (2.27), into Equation (2.32), the decision statistics can be found as,

$$\begin{aligned} \tilde{x}_1 &= (|h_1|^2 + |h_2|^2)x_1 + h_1^* n_1 + h_2 n_2^* \\ \tilde{x}_2 &= (|h_1|^2 + |h_2|^2)x_2 - h_1 n_2^* + h_2^* n_1. \end{aligned} \tag{2.33}$$

Finally, we can decide our symbols as given below:

$$\begin{aligned} \hat{x}_1 &= \arg\min_{\hat{x}_1 \epsilon \Omega} d^2(\tilde{x}_1, \hat{x}_1) \\ \hat{x}_2 &= \arg\min_{\hat{x}_2 \epsilon \Omega} d^2(\tilde{x}_2, \hat{x}_2). \end{aligned} \tag{2.34}$$

CHAPTER 3

ITERATIVE CHANNEL ESTIMATION FOR OFDM SYSTEMS

3.1. OFDM Channel Estimation

OFDM is an attractive multicarrier transmission approach for data transmission over frequency-selective fading channels. It has been already adopted in several wireless standards such as digital audio broadcasting (DAB), digital video broadcasting (DVB-T), IEEE 802.11a (IEEE 802.11a 1999) and Hiperlan/2 local area network (LAN) standard (ETSI 1998) (ETSI 1999), IEEE 802.16a metropolitan area network (MAN) standard (IEEE802.16 2001) and IEEE 802.20. Channel estimation is a very crucial task for OFDM systems. Accurate and robust channel estimation is necessary in order to demodulate the data coherently. Generally, it is assumed the channel state information (CSI), which is a mathematical value that represents a signal channel, is perfectly known at the receiver. However, in practice this is unlikely the case and the CSI is not known at the receiver and must be estimated by using estimation techniques. There are several channel estimation techniques used in the literature. These techniques can be classified as pilot-aided (Coleri et al. 2002) or blind channel estimation. In the pilot-aided channel estimation technique, a pilot sequence known at the receiver is embedded into the signal. At the receiver side, using these pilot symbols and the received signals, the channel is estimated. On the other hand, blind channel estimation techniques do not use any training symbols. They use the received signals and stochastic information (e.g., second order statics) of transmitted and received signals to estimate the channel coefficients. A widely used blind estimation technique is the subspace-based channel estimation. In this method, the autocorrelation matrix of the received data is decomposed into the signal and noise subspaces by using singular value decomposition (SVD) technique. Then, the channel can be estimated by using the orthogonality of the signal and noise. Compared to pilot aided techniques, blind techniques save on the use of pilots and can thus increase the spectral efficiency. However, blind techniques require prior knowledge of stochastic information

of the transmitted and received signals. Moreover, they always result in poorer performance compared to pilot-aided techniques. In this thesis, we will focus on pilot-aided channel estimation techniques.

In addition, researchers try different algorithms to improve the channel estimation accuracy of the OFDM systems. Expectation-Maximization (EM) Algorithm is one of those examples. This algorithm was first proposed by Dempster, Laird and Rubin in (Dempster et al. 1977). It has wide application areas such as channel estimation, signal detection, pattern recognition, neural network training, direction finding, image modelling and etc. In this thesis, the EM algorithm is used to improve the channel estimation performance.

The EM algorithm is a technique for finding maximum-likelihood (ML) estimation of system parameters in a broad range of problems where observed data are incomplete. The EM algorithm consists of two iterative steps: expectation (E) step and maximization (M) step. This algorithm is applied to the initial estimation results obtained using pilot symbols and these two steps of EM algorithm are iterated until the estimated values converge to the real channel (Ma et al. 2004).

In the following sections, the pilot-based and the EM-based channel estimation techniques and pilot-based iterative channel estimation technique with virtual subcarriers for OFDM systems will be explained in detail.

3.1.1. Pilot Based Channel Estimation

3.1.1.1. Overview

Pilot-based channel estimation is a widely used estimation technique due to its low computational complexity. The aim of this technique is to use distributed pilot symbols at certain locations in the OFDM time-frequency lattices to estimate the channel. In the estimation process, some estimation algorithms such as Least Squares (LS) and Minimum Mean Squared Error (MMSE) (Van de Beek et al. 1995) and interpolation techniques such as linear, spline, cubic, DFT-based etc. are exploited in time and frequency axes. We can examine these estimation algorithms by using the following general linear data model:

$$\mathbf{Y} = \mathbf{XH} + \mathbf{N}. \tag{3.1}$$

In this system our aim is to estimate channel matrix **H** with the knowledge of the received signal vector **Y** and transmitted signal vector **X**. The frequency domain channel matrix **H** is also expressed as **H=Fh**, where **F** is the fast fourier transform matrix and **h** is the time domain channel vector. Thus, the LS estimator is given as:

$$\hat{\mathbf{H}}_{LS} = \mathbf{X}^{-1}\mathbf{Y} \tag{3.2}$$

which minimizes $(\mathbf{Y} - \mathbf{XFh})^H(\mathbf{Y} - \mathbf{XFh})$. Without any knowledge of the statistics of the channels, the LS estimators are calculated with very low complexity, but they suffer from a high mean square error.

The MMSE estimator employs the second-order statics of the channel conditions to minimize the mean-square error. If the time domain channel vector **h** is Gaussian and uncorrelated with the channel noise **N**, the frequency domain MMSE estimate of **h** is given by

$$\hat{\mathbf{H}}_{MMSE} = \mathbf{F}\mathbf{R}_{hY}\mathbf{R}_{YY}^{-1}\mathbf{Y} \tag{3.3}$$

where

$$\begin{aligned}
\mathbf{R}_{hY} &= E\{\mathbf{hY}\} \qquad (3.4)\\
&= E\{\mathbf{h}(\mathbf{XFh} + \mathbf{N})^H\}\\
&= E\{\mathbf{hh}^H\mathbf{F}^H\mathbf{X}^H + \mathbf{hN}^H\}\\
&= \mathbf{R}_{hh}\mathbf{F}^H\mathbf{X}^H + E\{\mathbf{hN}^H\}\\
&= \mathbf{R}_{hh}\mathbf{F}^H\mathbf{X}^H\\
\mathbf{R}_{YY} &= E\{\mathbf{YY}\}\\
&= E\{(\mathbf{XFh+N})(\mathbf{XFh+N})^H\}\\
&= E\{\mathbf{XFhh}^H\mathbf{F}^H\mathbf{X}^H + \mathbf{XFhN}^H + \mathbf{Nh}^h\mathbf{F}^H\mathbf{X}^H + \mathbf{NN}^H\}\\
&= \mathbf{XFR}_{hh}\mathbf{F}^H\mathbf{X}^H + E\{\mathbf{NN}^H\}\\
&= \mathbf{XFR}_{hh}\mathbf{F}^H\mathbf{X}^H + \sigma_N^2\mathbf{I}_N
\end{aligned}$$

$\mathbf{R}_{hY}$ is the cross covariance matrix between **h** and **Y** and $\mathbf{R}_{YY}$ is the autocovariance matrix of **Y**. $\mathbf{R}_{hh}$ is the autocovariance matrix of **h** and σ_N^2 represents the noise variance.

The MMSE estimator yields a much better performance than LS estimator, especially under low Signal-to-Noise Ratio (SNR) conditions. A major drawback of the MMSE estimator is its high computational complexity.

As mentioned before, various interpolation techniques are used to estimate the channel matrix. The pilot-based channel estimation can be investigated in two categories according to the usage of these interpolation techniques in time or frequency axes. If we use interpolation in either time or frequency axes, our channel estimation is called one-dimensional (1D), if we use it both in time and frequency axes it is called two-dimensional (2D) channel estimation.

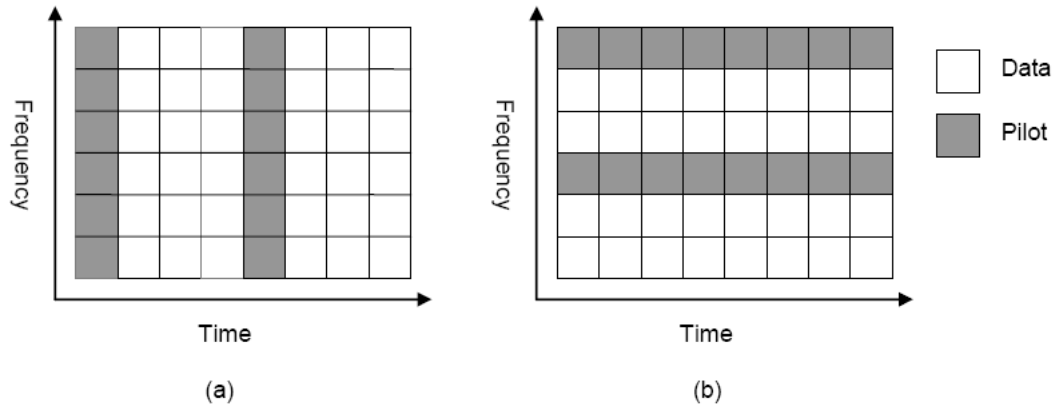

Figure 3.1. (a) Block type pilot arrangement. (b) Comb type pilot arrangement

The two basic 1D channel estimations in OFDM systems called block-type and comb-type are illustrated in Figure 3.1(a) and (b), respectively. The block-type channel estimation is performed by inserting pilot tones into all subcarriers of OFDM symbols. Thus, interpolation is performed only through the time axes. These kind of pilot structures are suitable for slow varying channel types. The second one, comb-type pilot channel estimation is suitable for fast fading channels. It is thus performed by inserting pilot tones into certain subcarriers of each OFDM symbol, therefore only frequency axes interpolation is performed (Coleri et al. 2002).

In the 2D channel estimation technique, pilot symbols are distributed at certain locations in time-frequency grid. The channel is estimated both in the time and the frequency axes. The pilots are spaced far from each other with a distance D_f in the frequency axes and D_t in the time axes. Mathematical expressions of the distances are given in Equations (3.5) and (3.6), respectively, where τ_d is the maximum delay spread, Δf is the minimum frequency spacing between two subcarriers, f_{dmax} is the maximum Doppler frequency and $T_{OFDM+CP}$ is the OFDM symbol duration. These distance conditions are

maintained for satisfying the sampling theorem.

$$D_f < \frac{1}{\tau_d \Delta f} \tag{3.5}$$

$$D_t < \frac{1}{2 f_{dmax} T_{OFDM+CP}}. \tag{3.6}$$

Instead of a 2D channel estimation, two 1D channel estimations can also be performed. Generally, performing two 1D estimations is preferred due to its simplicity compared to the 2D channel estimation. As seen in Figure 3.2, the interpolation techniques are applied in the time and the frequency axes, respectively in order to estimate the channel.

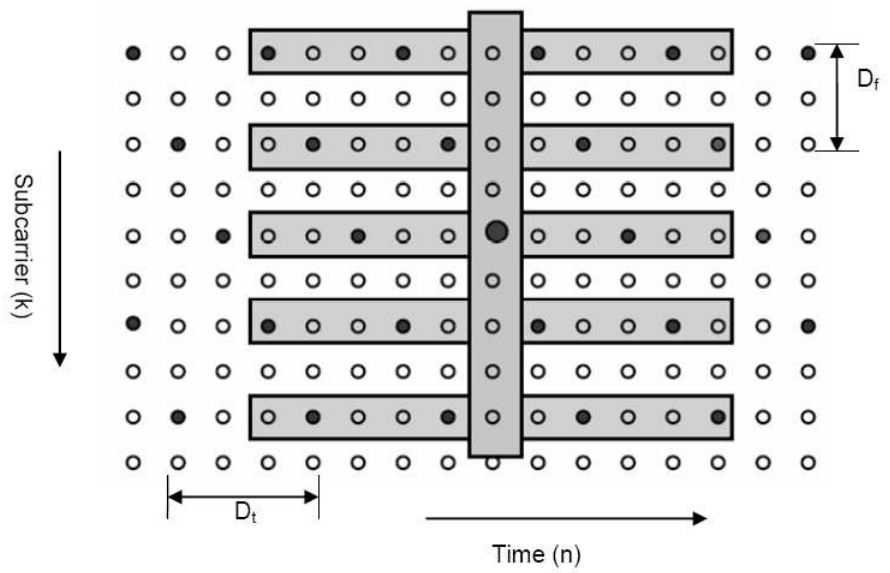

Figure 3.2. Two 1D pilot-based channel estimation

3.1.1.2. System Model

In the OFDM system model shown in Figure 3.3, after the data is modulated, pilot symbols are inserted into the complex data. At the receiver side, these pilot symbols are extracted and used for the channel estimation. Using the received signals at pilots position, LS channel estimation algorithm can be performed in the frequency domain as:

$$\hat{H}_n(k) = \frac{Y_n(k)}{X_n(k)} = H_n(k) + \frac{N_n(k)}{X_n(k)}, \tag{3.7}$$

where k and n represent the places of pilot symbols in the frequency and the time axes respectively and $\hat{H}_n(k)$ are the estimated channel coefficients belonging to the pilot subcarriers. The estimation error is calculated as $\sigma_{ch}^2 = 2\sigma_N^2$ when the pilot and data symbols have normalized power.

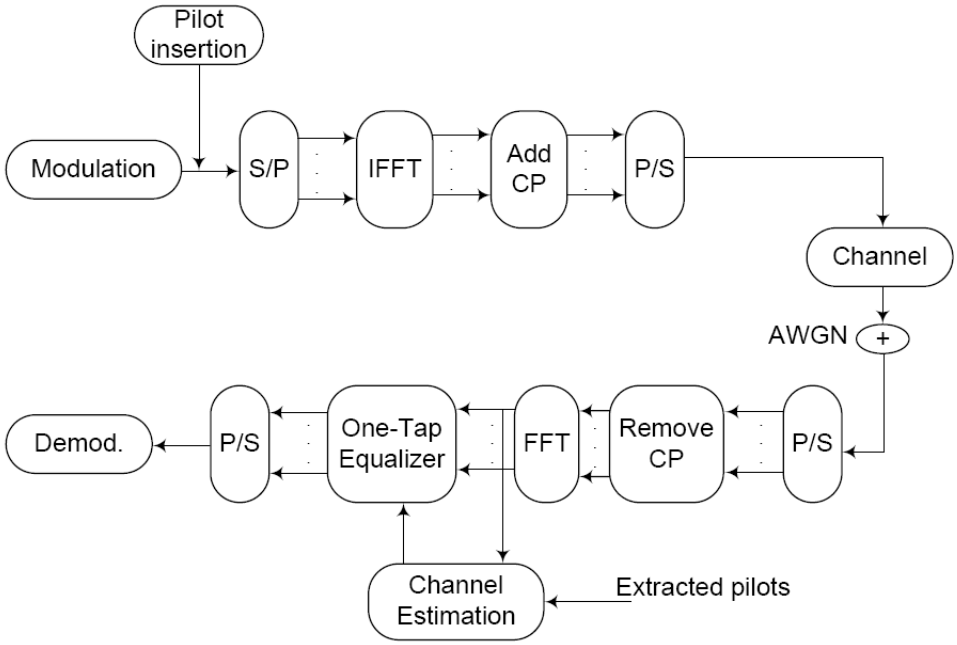

Figure 3.3. OFDM Block diagram with channel estimation

The estimated channel vector can be reconstructed for each OFDM symbol $\hat{\mathbf{H}}_n = [\hat{H}_n(1), \hat{H}_n(D_f+1), ..., \hat{H}_n((N_f-1)D_f+1)]^T$ where D_f is the distance between the subcarriers and N_f is the number of pilot symbols in the frequency axes. We use DFT-based interpolation technique in the frequency axes in order to estimate all channel coefficients belonging to all subcarriers. First, we transform the frequency channel estimate $\hat{\mathbf{H}}_n$ into time domain as:

$$\hat{\mathbf{h}}_n = \mathbf{F}^{-1}\hat{\mathbf{H}}_n \tag{3.8}$$

where $\mathbf{F}$ is the $N_f \times N_f$ DFT matrix. Then we apply a filtering matrix to $\hat{\mathbf{h}}_n$ assuming that the channel response is limited to L_f and obtain the filtered channel response

$$\hat{\mathbf{h}}_n^{(0)} = \mathbf{W}\hat{\mathbf{h}}_n. \tag{3.9}$$

For the above equation $\mathbf{W}$, is the $L_f \times N_f$ filtering matrix. Then we apply DFT in order to obtain the initial estimates for the nth OFDM symbol

$$\hat{\mathbf{H}}_n^{(0)} = \mathbf{V}\hat{\mathbf{h}}_n^{(0)}, \tag{3.10}$$

where **V** is the $K \times L_f$ matrix obtained from the first L_f columns of the $K \times K$ DFT matrix.

In order to estimate the other channel cofficients in the frame, we simply apply linear interpolation in the time domain using the estimated channel coefficients for each subcarrier. As a result, all estimated channel coefficients in the frame is obtained to reconstruct the data symbols using simple one-tap frequency domain equalizer as:

$$\tilde{X}_n(k) = \frac{Y_n(k)}{\hat{H}_n^{(0)}(k)}. \tag{3.11}$$

Then, we can decide the transmitted symbols $\hat{X}_n(k)$ by using the Equation (2.34).

3.1.2. Expectation-Maximization (EM) Based Channel Estimation

3.1.2.1. Overview

The EM algorithm is an iterative method for solving the ML estimation problems in the presence of unobserved data. The aim of this algorithm is to augment the observed data with the hidden data so that it will be easy to manipulate the likelihood function conditioned on the data and the hidden data. The algorithm consists of two major steps: an expectation step (E-step) followed by a maximization step (M-step). We can divide our complete data Z into two components such as $Z = (X, Y)$, where X are the observed data or incomplete data and Y are the hidden data or the missing data. We will try to estimate an unknown paramater denoted as Θ by using the missing data Y (Moon 1996).

According to the EM procedure E-step finds $Q(\Theta|\Theta^{(p)})$, the expected value of the loglikelihood of the Θ. The expectation is taken with respect to Y conditioned on X and $\Theta^{(p)}$, the latest estimate of the Θ:

$$Q(\Theta|\Theta^{(p)}) = E\{\log f(Z|\Theta)|X, \Theta^{(p)}\} \tag{3.12}$$

where p is the iteration number. We can find the $\Theta^{(p+1)}$, which maximizes $\Theta^{(p)}$ over all possible values of Θ,

$$\Theta^{(p+1)} = \arg\max_{\theta} Q(\Theta|\Theta^{(p)}). \tag{3.13}$$

These two steps are iterated until $\Theta^{(p)}$ converges to the ML estimate of Θ.

3.1.2.2. System Model

First we will derive the formulas for one OFDM symbol in an OFDM frame. Thus, we will ignore time index n in the equations. According to the Gaussian noise assumption, the probability density function (pdf) of $Y(k)$ given $X(k)$ and $H(k)$ is given by

$$f(Y(k)|X(k),H(k)) = \frac{1}{\sqrt{2\pi\sigma^2}} \exp\left\{-\frac{1}{2\sigma^2}|Y(k) - H(k)X(k)|^2\right\}. \tag{3.14}$$

When the transmitted signal $X(k)$ is QPSK modulated we can denote the symbols in the signal constellation by $X_i, 1 \leqslant i \leqslant C$, where C is equal to 4. The value of C changes according to the modulation type. The pdf of $Y(k)$ given $H(k)$ is obtained by assuming that all C symbols are equally likely and averaging the conditional pdf of Equation (3.14) over the variable $X(k)$ as follows:

$$f(Y(k)|H(k)) = \sum_{i=1}^{C} \frac{1}{\sqrt{2\pi\sigma^2 C}} \exp\left\{-\frac{1}{2\sigma^2}|Y(k) - H(k)X_i|^2\right\}. \tag{3.15}$$

Until now we presented the equations assuming only one OFDM symbol in an OFDM frame. However, we can transform the equations into a general form by assuming more OFDM symbols in an OFDM frame. It can be supposed that the channel is static over the period of N OFDM symbols. We define the received signal vector for a subcarrier along N symbols $\mathbf{Y} = [Y_1(k), ..., Y_N(k)]$ and the transmitted signal vector $\mathbf{X} = [X_1(k), ..., X_N(k)]$. Then using the procedure of the EM algorithm, we denote $\mathbf{Y}$ and $(\mathbf{Y}, \mathbf{X})$ as incomplete data and complete data, respectively. We can write the conditional pdf of the incomplete data by assuming that additive Gaussian noise is independent from symbol to symbol for each subcarrier as follows:

$$f(\mathbf{Y}|H_n(k),\mathbf{X}) = \prod_{n=1}^{N} f(Y_n(k)|H_n(k),X_n(k)). \tag{3.16}$$

Thus the loglikelihood function of the incomplete data is

$$\log f(\mathbf{Y}|H_n(k),\mathbf{X}) = \sum_{n=1}^{N} \log f(Y_n(k)|H_n(k),X_n(k)) \tag{3.17}$$

and the loglikelihood function of complete data $(\mathbf{Y}, \mathbf{X})$

$$\log f(\mathbf{Y},\mathbf{X}|H_n(k)) = \sum_{n=1}^{N} \log\left\{\frac{1}{C} f(Y_n(k)|H_n(k),X_n(k))\right\}. \tag{3.18}$$

We try to find an estimate of $H_n(k)$ that maximizes $f(\mathbf{Y}, H_n(k))$ in ML estimation. However, as seen in Equation (3.17) it is not easy to manipulate the summation of several exponential functions, so we use EM algorithm in order to increase the likelihood at each step. Each iterative process $p = 0, 1, 2, ...$ in the EM algorithm for estimating $H_n(k)$ from $\mathbf{Y}$ consists of the following two iterative steps:

E-Step:

$$\Theta(H_n(k)|H_n^{(p)}(k)) = E_{\mathbf{X}}\{\log f(\mathbf{Y}, \mathbf{X}|H_n(k))|\mathbf{Y}, H_n^{(p)}(k)\}$$

$$\begin{aligned} &= \sum_{i=1}^{C}\sum_{n=1}^{N} \log\left\{\frac{1}{C} f(Y_n(k)|H_n(k), X_i)\right\} f(X_i|Y_n(k), H_n^{(p)}(k)) \qquad (3.19)\\ &= \sum_{i=1}^{C}\sum_{n=1}^{N} \log\left\{\frac{1}{C} f(Y_n(k)|H_n(k), X_i)\right\} \frac{f(Y_n(k)|H_n^{(p)}(k), X_i) f(X_i|H_n^{(p)}(k))}{f(Y_n(k)|H_n^{(p)}(k))}\\ &= \sum_{i=1}^{C}\sum_{n=1}^{N} \log\left\{\frac{1}{C} f(Y_n(k)|H_n^{(p)}(k), X_i)\right\} \frac{f(Y_n(k)|H_n^{(p)}(k), X_i)}{C f(Y_n(k)|H_n^{(p)}(k))} \end{aligned}$$

M-Step:

$$\begin{aligned} \hat{H}_n^{(p+1)}(k) &= \arg\max_{H_n(k)} \Theta(H_n(k)|H_n^{(p)}(k)) \qquad (3.20)\\ &= \arg\max_{H_n(k)} \sum_{i=1}^{C}\sum_{n=1}^{N} \log\{f(Y_n(k)|H_n^{(p)}(k), X_i)\} \frac{f(Y_n(k)|H_n^{(p)}(k), X_i)}{f(Y_n(k)|H_n^{(p)}(k))}\\ &= \arg\min_{H_n(k)} \sum_{i=1}^{C}\sum_{n=1}^{N} |Y_n(k) - X_i H_n(k)|^2 \frac{f(Y_n(k)|H_n^{(p)}(k), X_i)}{f(Y_n(k)|H_n^{(p)}(k))} \end{aligned}$$

Then differentiating the last expression with respect to $H_n(k)$, and setting it to zero, we have:

$$\hat{H}_n^{(p+1)}(k) = \frac{\sum_{i=1}^{C}\sum_{n=1}^{N} Y_n(k) X_i^* \frac{f(Y_n(k)|H_n^{(p)}(k), X_i)}{f(Y_n(k)|H_n^{(p)}(k))}}{\sum_{i=1}^{C}\sum_{n=1}^{N} |X_i|^2 \frac{f(Y_n(k)|H_n^{(p)}(k), X_i)}{f(Y_n(k)|H_n^{(p)}(k))}}. \qquad (3.21)$$

The channel estimate in Equation (3.21) obtained for the K subcarriers can be refined by the filtering operations given in Equations (3.9) and (3.10). The same filtering procedure can also be realized by applying the IFFT followed by FFT, as illustrated in Figure 3.4. The values $h_n^{(p+1)}(l)$, $L \leqslant l \leqslant K-1$ obtained by the IFFT must be set to zero before FFT process where L shows the number of taps of the channels. Thus, the estimation noise from paths that do not actually exist is eliminated.

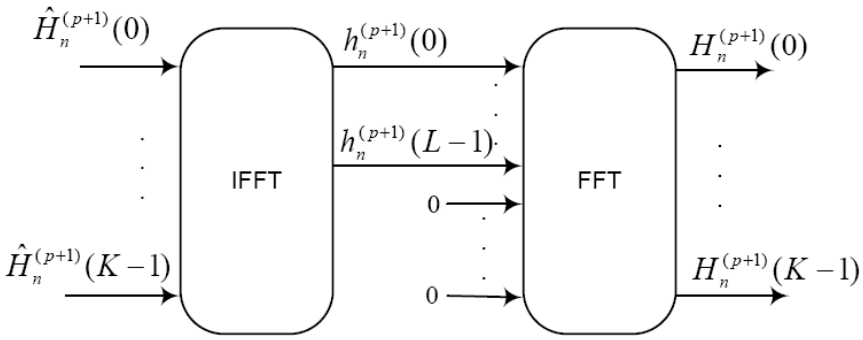

Figure 3.4. Lowpass filter structure

The iterative procedure is terminated as soon as the difference between $\mathbf{H}^{(p+1)}$ and $\mathbf{H}^{(p)}$ is sufficiently small. After getting the frequency domain channel response $\hat{H}_n(k)$, the ML estimate of the transmitted signal can be found as:

$$\hat{X}_n(k) = \arg\min_{X \epsilon C} |Y_n(k) - \hat{H}_n(k) X_n(k)|^2, \qquad 0 \leqslant k \leqslant K-1. \tag{3.22}$$

3.1.3. The Proposed Pilot-based iterative channel estimation

The channel estimation accuracy can be improved by adding virtual pilots using an iterative channel estimation and data detection. The hard decision symbols $\hat{X}_n(k)$ can be used as virtual pilots. Thus, there will be an iteration between the decision and the channel estimation block at the receiver, which is a kind of decision feedback equalization technique, as seen in Figure 3.5.

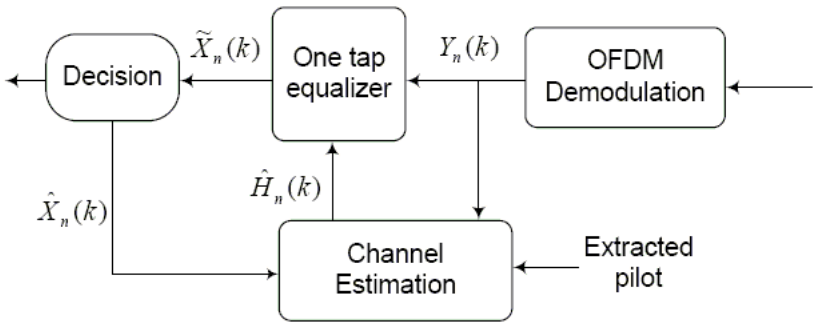

Figure 3.5. OFDM receiver for proposed iterative channel estimation

The LS channel estimation is calculated with the new virtual pilot symbols and then interpolation techniques such as DFT-based interpolation is applied. These LS estimates can be divided into groups that contains N_f equally spaced estimates before applying the interpolation. Thus, $K/N_f - 1$ virtual pilot groups $\hat{\mathbf{H}}_{g,n} = [\hat{H}_n(g), \hat{H}_n(D_f + g), ..., \hat{H}_n((N_f - 1)D_f + g)]^T$ are obtained as seen in Figure 3.6. For each group, a DFT-based interpolation is performed considering their corresponding delays as:

$$\hat{\mathbf{h}}_{g,n} = \mathbf{F}^{-1}\hat{\mathbf{H}}_{g,n}\mathbf{D}_g \tag{3.23}$$

where $\mathbf{D}_g = e^{j2\pi(g-1)[0:N_f-1]/K}$ for $g = 2, 3, ..., K/N_f$.

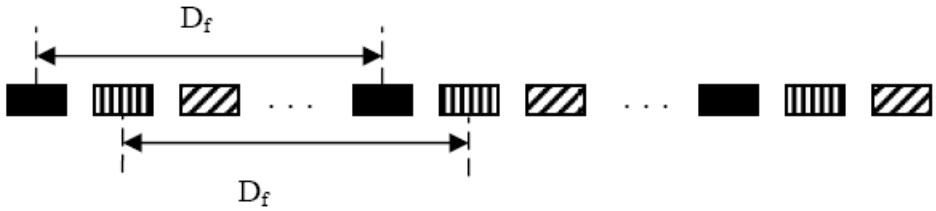

Figure 3.6. Group representation

Instead of averaging the group estimates, we propose to combine them by taking into account their reliability that is calculated by using the pdf of Y given X and H. This probability for each subcarrier can be found as:

$$f(Y_n(k)|\hat{X}_n(k), \hat{H}_n^{(0)}(k)) = \frac{1}{\sqrt{2\pi\sigma^2}} \exp\left\{-\frac{1}{2\sigma^2}|Y_n(k) - \hat{H}_n^{(0)}(k)\hat{X}_n(k)|^2\right\}. \tag{3.24}$$

For $P_n(k) = f(Y_n(k)|\hat{X}_n(k), \hat{H}_n^{(0)}(k))$, the reliability of the hard-decision symbols can be divided into $K/N_f - 1$ groups such as $\mathbf{P}_{g,n} = [P_n(g), P_n(D_f + g), ..., P_n((N_f - 1)D_f + g)]^T$. From this predicted probability, we estimate the probability of correctness of the associated group and can define the reliability factor of each group as:

$$P_{rel}(g) = \prod_{m=1}^{N_f} (P_n(g + D_f(m - 1))). \tag{3.25}$$

As a result the combining stage is performed by (Özbek et al. 2005):

$$\hat{\mathbf{h}}_n^{(1)} = \frac{\hat{\mathbf{h}}_n^{(0)} + \sum_{g=2}^{K/N_f} P_{rel}(g)\hat{\mathbf{h}}_{g,n}}{1 + \sum_{g=2}^{K/N_f} P_{rel}(g)}. \tag{3.26}$$

Then, $\hat{\mathbf{H}}_n^{(1)}$ can be calculated as

$$\hat{\mathbf{H}}_n^{(1)} = \mathbf{V}(\mathbf{W}\hat{\mathbf{h}}_n^{(1)}). \tag{3.27}$$

After getting the new channel estimates, the transmitted symbols are estimated at the second iteration by using the Equation (3.11).

3.1.4. Channel Estimation Performance Comparison for Different Pilot Arrangements

While performing a channel estimation, the complexity of the system and the number of the pilot symbols, used for the channel estimation, are two important points to be considered. For the pilot-aided channel estimation, the number of the pilots and the performance of the system is always a tradeoff. Using too many pilots for having a good performance causes to use spectrum inefficiently. Thus, the arrangements of the pilots in the time-frequency lattices is an important design problem.

In this section, two methods, which have different pilot arrangements in the time-frequency lattices and different number of pilot symbols in a frame, are compared. Pilot-aided channel estimation is used for the initial estimation and EM algorithm is used to increase the estimation performance for both methods (Baştürk and Özbek 2007). In practise the number of taps in the channel is an unknown parameter and must be estimated. However, in this study it is assumed that the number of the taps of the channel is known for both methods.

Method 1: In the first method, which we named distributed, the pilot symbols are distributed at certain locations in the OFDM time-frequency lattices to find appropriate initial values. The pilot arrangement structure is shown in Figure 3.7. The channel estimation process for this method can be given as follows. Firstly, the simple LS algorithm given in Equation (3.2) is used to obtain channel frequency response at pilot positions. Then, two 1D interpolation technique is used to find all the elements of the channel

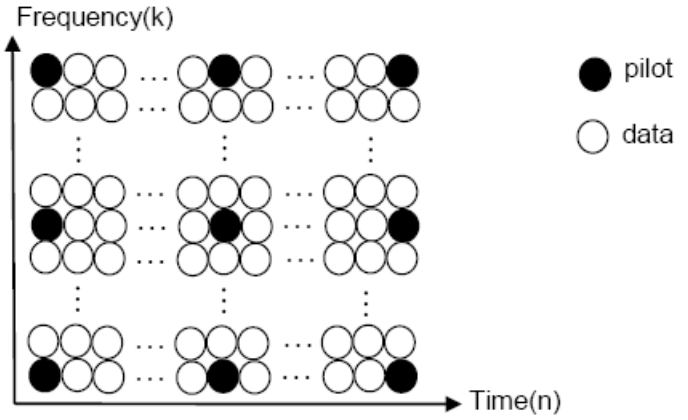

Figure 3.7. Pilot arrangement in the time-frequency lattices for Method 1

matrix. In the frequency axes DFT- based interpolation and in the time axes linear interpolation is applied respectively. So, the initial channel estimation is obtained for this method. EM algorithm is applied to these channel coefficients individually to improve the estimation performance. Then, the output of the EM algorithm is passed through a low-pass filter in order to refine the channel estimation performance as shown in Figure 3.4. In this method, 64 OFDM symbols are used in one OFDM frame. Also, one OFDM frame consists of uniform spacing of 64 pilot symbols with $D_t = 9$ in the time axes and with $D_f = 8$ in the frequency axes and 4032 data symbols. Thus the overhead caused by pilot symbols is only 1/64. Interpolation techniques are performed both in the time and the frequency axes for this method.

Method 2: For the second method, which we named as sequential channel estimation, the pilot arrangement in OFDM time-frequency lattices is seen in Figure 3.8. The pilot symbols are inserted into only the first OFDM symbol. So the first aim is to estimate the channel coefficients of the first OFDM symbol. The frequency response at pilot positions is found by using LS algorithm again. Then, DFT-based interpolation at frequency axes is applied in order to estimate all channel coefficients belonging to this OFDM symbol. After getting the channel estimation vector, the EM algorithm and filtering processes are applied in order to increase the estimation performance. For estimating next symbol's channel coefficients the channel estimates belonging to the previous symbol is used as the initial estimate and the EM algorithm is applied. This process is repeated in order to estimate all channel coefficients for OFDM frame. In this method again 64 OFDM symbols

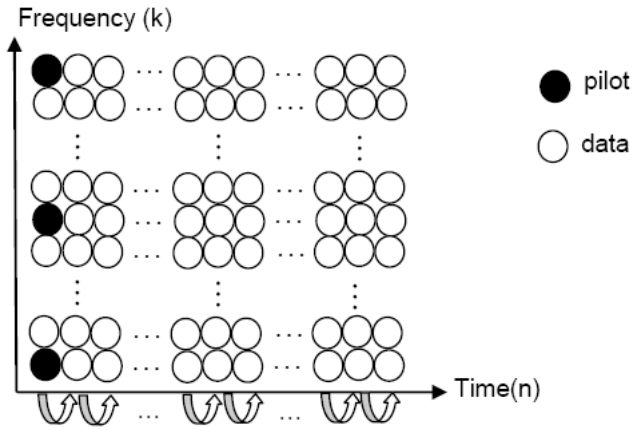

Figure 3.8. Pilot arrangement in the time-frequency lattices for Method 2

are used in one OFDM frame. However, 8 pilot symbols and 4088 data symbols are used for a frame and only frequency domain interpolation is performed.

3.1.4.1. Simulation Results

For these OFDM systems, the entire channel bandwidth is chosen as 800 kHz, and divided into 64 subcarriers. To make the subcarriers orthogonal to each other, the symbol duration is chosen as 80 microseconds. The length of the CP we used is 20 microseconds and this means $N_{cp} = 16$. Thus, the total OFDM symbol time is $T_{OFDM+CP} = 100\mu s$. The modulation type used in these systems is QPSK. The maximum doppler frequency f_{dmax} is chosen as 100 Hz, which implies $f_{dmax}T_{OFDM+CP} = 0.01$. The CIR used in this study is:

$$h(n) = \frac{1}{Z}\sum_{l=0}^{7} e^{-l/2}\alpha_l \delta(n-l) \tag{3.28}$$

where $Z = \sqrt{\Sigma_{l=0}^{7} e^{-l}}$ is the normalization constant and α_l, $0 \leqslant l \leqslant 7$, are independent complex-valued Gaussian random variables with unit variance, which vary in time according to the Doppler frequency. The amplitudes of α_l are Rayleigh distributed. This is a conventional exponential decay multipath channel model. All simulation results are obtained using MATLAB.

Figure 3.9 shows the BER performance comparison of the EM algorithm and pilot-based initial estimation. It is observed that the EM algorithm reduces the BER compared to only pilot-based estimation.

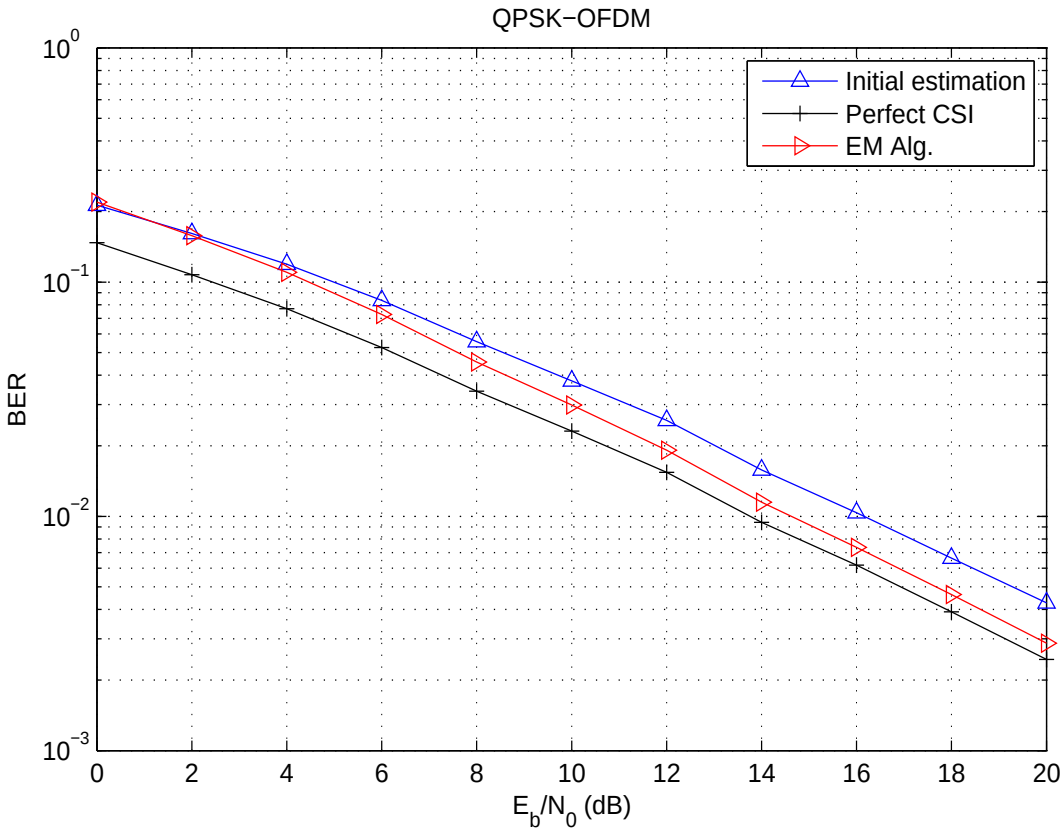

Figure 3.9. BER versus E_b/N_0 for QPSK-OFDM

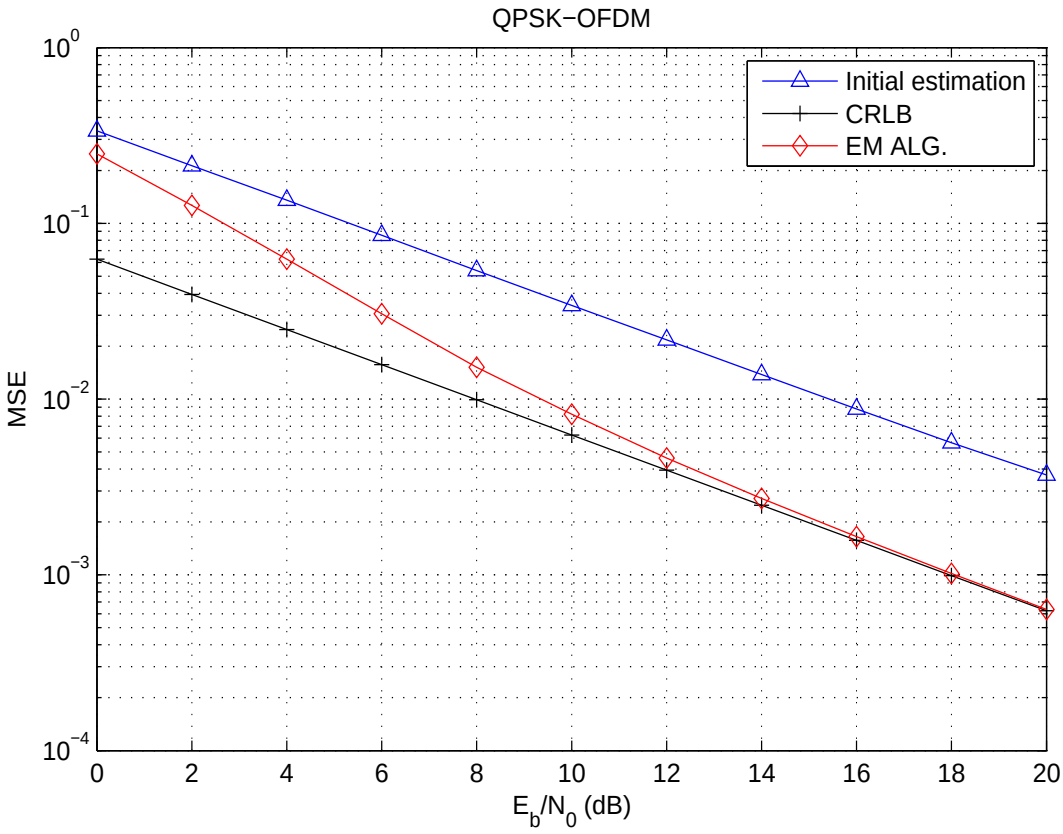

Figure 3.10. MSE versus E_b/N_0 for QPSK-OFDM

From Figure 3.10 we can see the channel estimation performance of the EM algorithm and pilot-based initial estimation. Again, EM algorithm is better than initial estimation and especially after 14 dB it is very close the Cramer-Rao Lower Bound (CRLB), which expresses a lower bound on the variance of estimators of a deterministic parameter. These figures show us that the EM algorithm improve the channel estimation performance. Method 1 is used to compare these two estimation algorithms.

After we compared the pilot-aided initial channel estimation and EM algorithm, the performance of the two methods which have different pilot arrangements and different number of pilots are examined in terms of BER, MSE and the number of iterations used in the EM algorithm. The BER results are given in Figure 3.11. In this figure, we can see that Method 1 and Method 2 gives approximately the same performance above 16 dB.

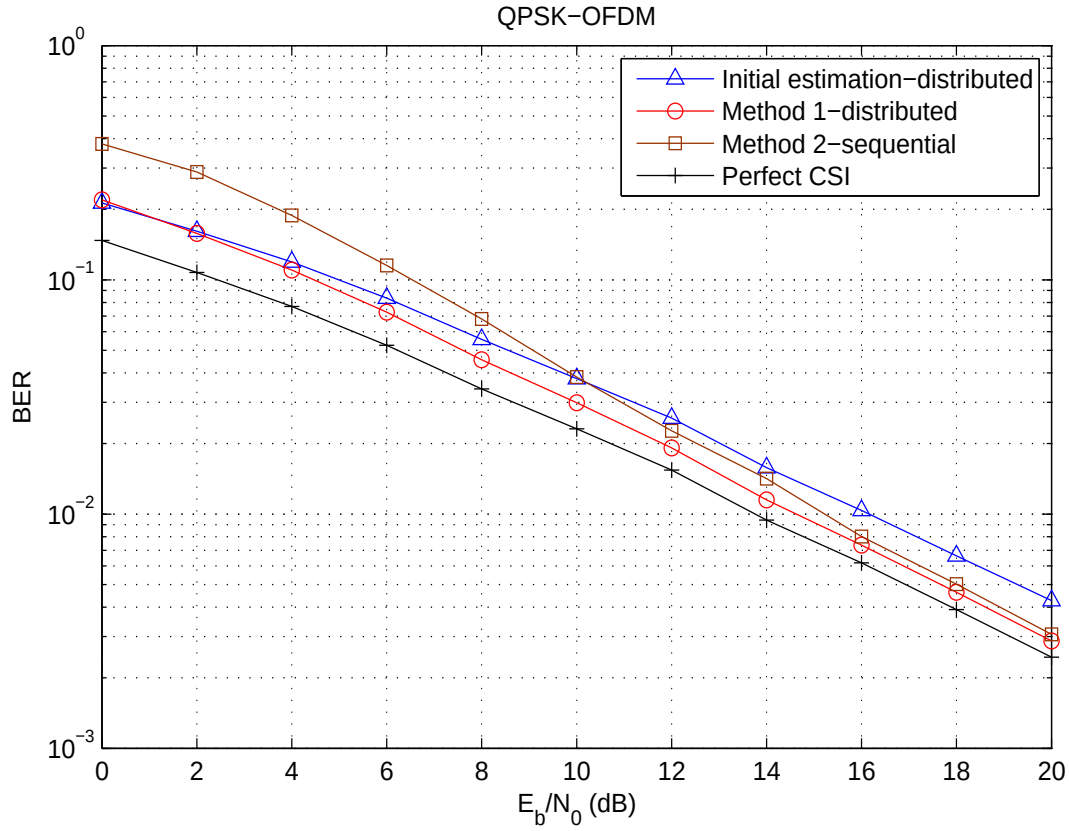

Figure 3.11. Comparison of BER for two methods

According to the MSE results seen in Figure 3.12, Method 1 almost achieves CRLB in the high E_b/N_0 region. Especially, it is very close to the CRLB, when E_b/N_0 >14 dB. The performance of Method 2 is again better than the initial estimation and getting closer to the Method 1 when E_b/N_0 >14 dB.

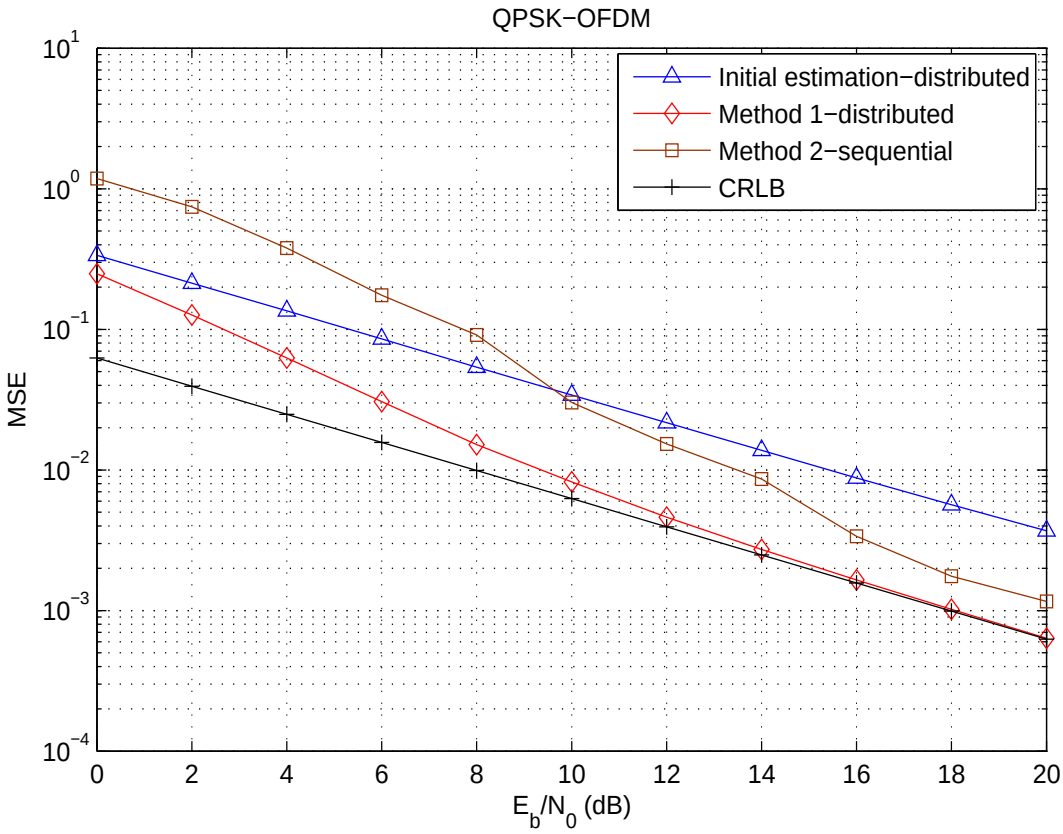

Figure 3.12. Comparison of channel estimation performance for two methods

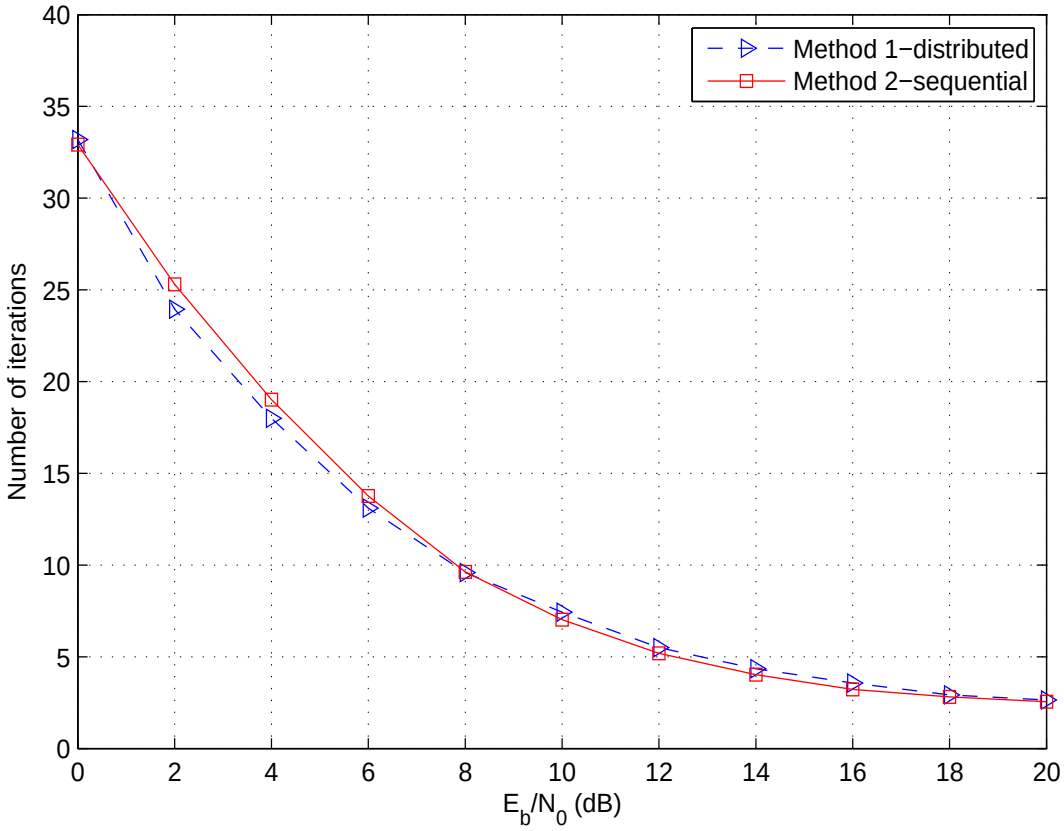

Figure 3.13. Comparison for number of iterations

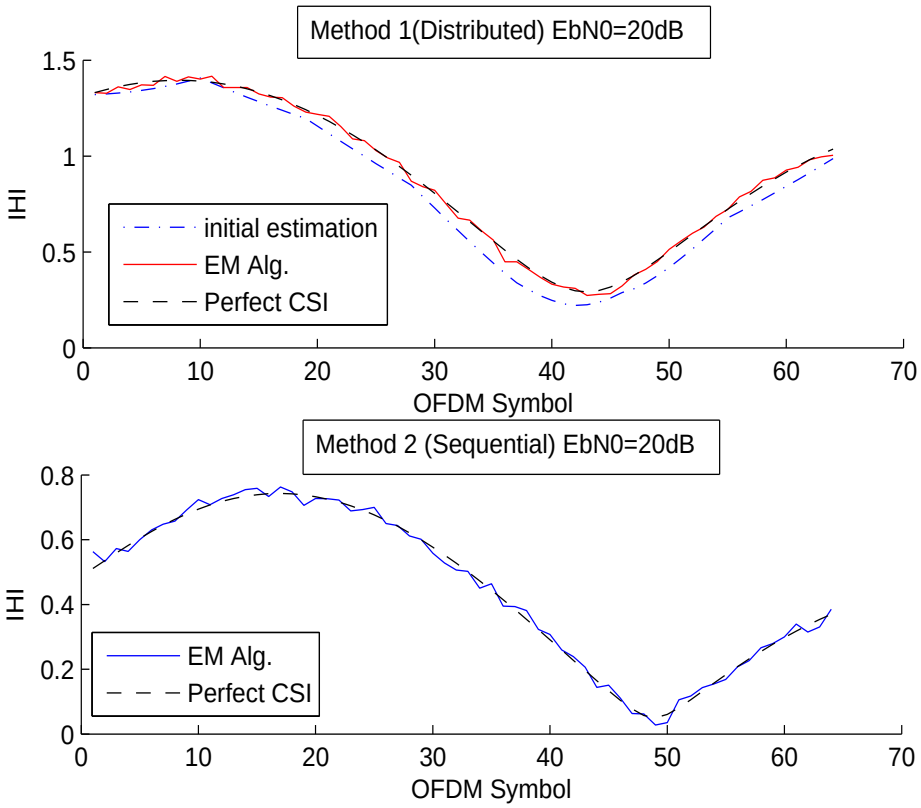

Figure 3.14. Tracking channel variations in time for Method 1 and Method 2

The number of iterations used in the EM algorithm is compared for both pilot arrangements in Figure 3.13 in order to compare the complexity of the systems. The results are almost the same for both methods. However, Method 2 has lower complexity since time domain interpolation is not performed. The comparison of two methods is given below in Table 3.1.

Table 3.1. Comparison of Method 1 and Method 2

	Method 1(Distributed)	Method 2(Sequential)
Number of pilot symbols in a frame	64	8
Frequency axes interpolation	DFT-based	DFT-based
Time axes interpolation	Linear interpolation	No interpolation
Number of iterations used in EM (E_b/N_0=10 dB)	7	7
Number of iterations used in EM (E_b/N_0=20 dB)	2	2
Normalized simulation duration for one OFDM frame	1	0.67

As a result, we can say that the performance of the Method 2, which contains less pilot symbols, is almost the same as the performance of the Method 1 after passing a low SNR threshold with lower complexity. Finally, we also showed how the channel variations are being tracked in time for both methods in Figure 3.14. From this figure, it is seen that for both methods EM algorithm tracks the channel variations perfectly.

We also compared the BER and the MSE performance of the proposed iterative channel estimation with virtual pilot symbols as defined in section 3.1.3 and Method 1 as seen in Table 3.2. The simulation parameters and the channel type are the same as used in Method 1. Instead of the EM algorithm, the channel estimation performance is improved by using virtual pilot subcarriers. The pilot symbols are distributed in the time-frequency lattices as seen in Figure 3.7. Firstly, an initial channel estimation is performed by using these pilot symbols and transmitted symbols are decoded. Then, hard decision symbols are obtained by using these symbols. These symbols are sent back to the channel estimation block as virtual pilot symbols. After that, a new channel estimation

Table 3.2. Comparison of Method 1 and Proposed pilot-aided algorithm

	Method 1	Proposed pilot aided
Number of pilot symbols in a frame	64	64
Frequency axes interpolation	DFT-based	DFT-based
Time axes interpolation	Linear interpolation	Linear interpolation
Number of iterations used in EM (E_b/N_0=10 dB)	7	1
Number of iterations used in EM (E_b/N_0=20 dB)	2	1
Normalized simulation duration for one OFDM frame	1	0.34

is performed as proposed in Equation (3.26) and (3.27) respectively. The transmitted symbols are decoded by using these channel coefficients again.

Figure 3.15 and 3.16 show the BER and the MSE performance comparison for two methods. According to these figures, it is seen that the BER performance for the iterative method and EM algorithm is almost the same. Moreover, the channel estimation performance for two methods is also very close. Both of them have better performance than initial channel estimation which is obtained by pilot symbols. The iterative channel estimation method has lower computational complexity because EM algorithm performs many inner iterations for low SNR values.

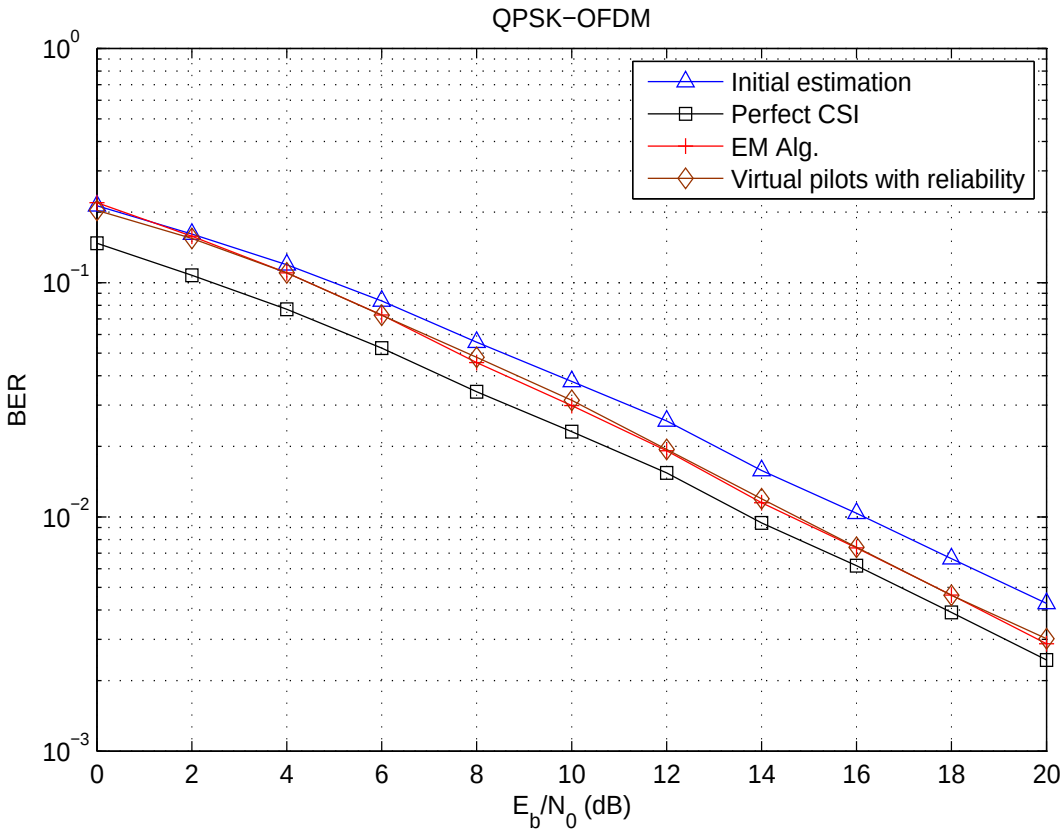

Figure 3.15. BER comparison of the proposed and EM algorithm

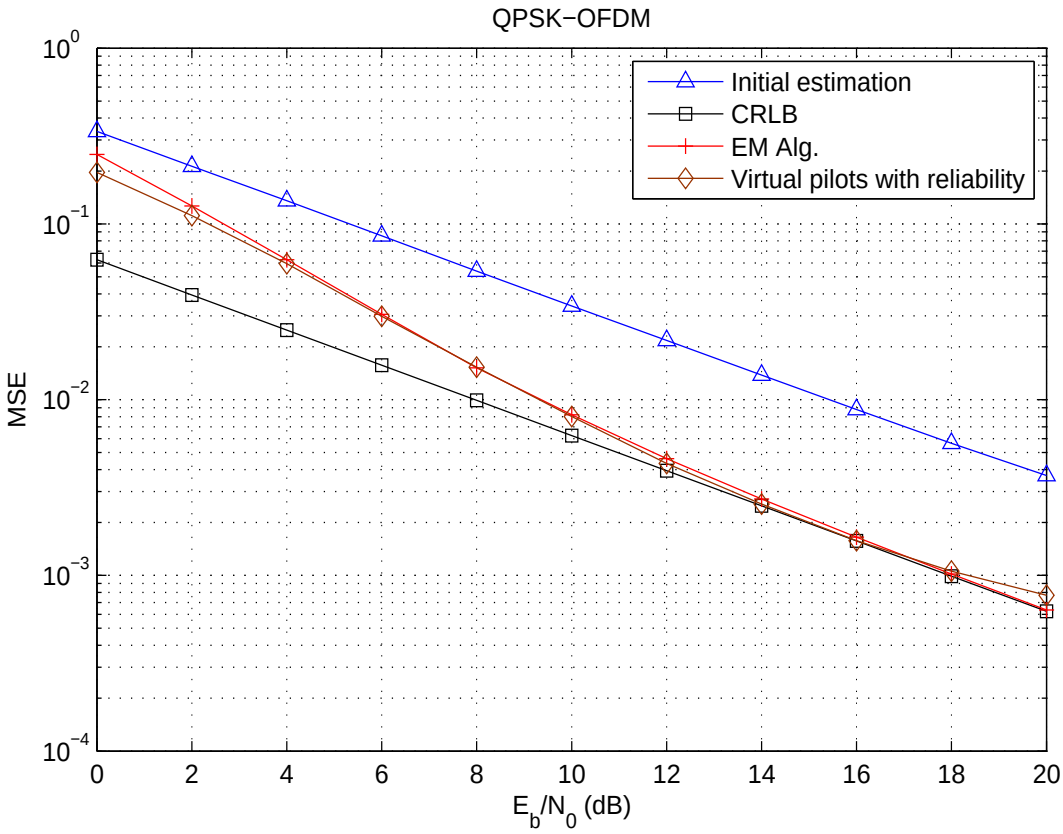

Figure 3.16. MSE performance comparison of the proposed and EM algorithm

CHAPTER 4

ITERATIVE CHANNEL ESTIMATION FOR MIMO-OFDM SYSTEMS

OFDM has been successfully applied to a wide variety of wireless communication systems such as wireless local area network (WLAN) systems due to its capability to effectively combat ISI, and its spectral efficiency achieved by spectrum overlapping. MIMO systems with multiple antennas at both transmit and receive sides have the ability to improve spectral efficiency, link reliability, coverage or capacity. Therefore, the combination of MIMO and OFDM is a strong candidate for the future wireless communication systems. In this chapter MIMO-OFDM system model and channel estimation, STBC-OFDM and V-BLAST structured OFDM will be examined by giving simulation studies.

4.1. MIMO-OFDM System Model

A MIMO-OFDM system model with N_t transmit antennas and N_r receive antennas is shown in Figure 4.1. At the transmission time n, a binary data block **b** is modulated and then passed through the serial-to-parallel converter and a complex data matrix **S** with a lenght $K \times N$ is obtained, where N is the total number of OFDM symbols and K is the total number of subcarriers. Then the complex data is passed through the MIMO encoder to produce N_t data streams, $X_i[n,k]$ for $i = 1, ..., N_t$, for transmission over the multiple antennas. Each of these signals forms an OFDM block. These signals are passed through IFFT block and then CP is added to mitigate ISI. The transmit antennas simultaneously transmit these OFDM signals. Assuming the channel impulse response remains constant during the entire OFDM block, the received signal vector that belongs to the jth receive antenna, is simply the linear convolution of transmitted symbols and the channel impulse response vector. At the receiver, the signals from N_t transmit antennas are superimposed and the output of FFT at the jth receive antenna can be expressed as;

$$Y_j(n,k) = \sum_{i=1}^{N_t} X_i(n,k) H_{ij}(n,k) + N_j(n,k) \tag{4.1}$$

where $H_{ij}(n,k)$ denotes the channel frequency response at time n for the kth subcarrier between the ith transmit and jth receive antennas. $N_j(n,k)$ represents the AWGN with zero mean and σ_N^2 variance.

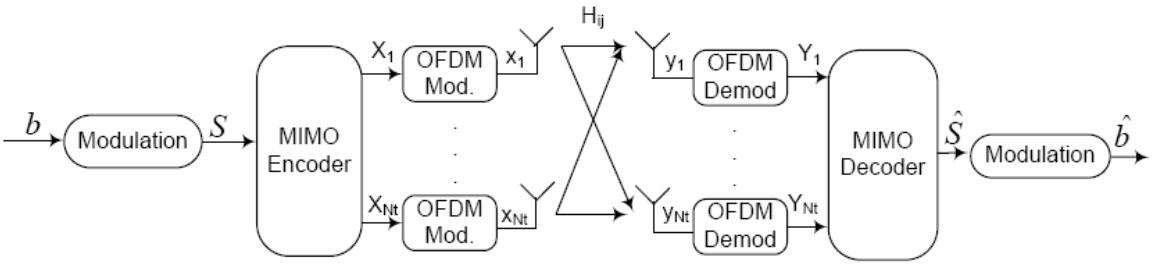

Figure 4.1. MIMO-OFDM System Model

The time-domain channel impulse response between the jth receive antenna and the ith transmit antenna can be modelled as a tapped-delay line. With only the non-zero taps considered, it can be expressed as

$$h_{ij}(t,\tau) = \sum_{l=1}^{L_t} \alpha_{ij,l}(t)\delta(\tau - \frac{n_l}{K\Delta f}) \tag{4.2}$$

where $\delta(.)$ is the Dirac delta function, L_t denotes the number of non-zero taps, $\alpha_{ij,l}(t)$ is the complex amplitude of the lth non-zero tap, whose delay is $\frac{n_l}{K\Delta f}$, where n_l is an integer and Δf is subcarrier spacing of the OFDM system. The channel frequency response between the jth receive antenna and the ith transmit antenna which belongs to the kth subcarrier and the nth OFDM symbol can be obtained by taking the Fourier transform and can be expressed as;

$$\begin{aligned} H_{ij}(k,n) = H_{ij}(nT_{OFDM+CP}, k\Delta f) &= \sum_{l=1}^{L_t} \alpha_{ij,l}(nT_{OFDM+CP}) e^{-j2\pi \frac{k}{K} n_l} \\ &= \mathbf{h}_{ij}^H(n)\mathbf{w}_f(k) \end{aligned} \tag{4.3}$$

where $T_{OFDM+CP}$ is the OFDM symbol duration with CP, $\mathbf{h}_{ij}(n) = [\alpha_{ij,1}(nT_{OFDM+CP}), ..., \alpha_{ij,L_t}(nT_{OFDM+CP})]^H$ is the L_t sized vector containing the time responses of all the nonzero taps, $\mathbf{w}_f(k) = [e^{-j2\pi \frac{k}{K} n_1}, ..., e^{-j2\pi \frac{k}{K} n_{L_t}}]^T$ contains corresponding FFT coefficients (Lu and Wang 2000).

4.2. Space-Time Coded OFDM Systems

STC is designed to extract spatial diversity from flat fading MIMO channels. The STC systems can provide significant capacity gains in wireless channels. However the STC design becomes a complicated issue because many practical wireless channels are frequency-selective in nature. The system design problem for MIMO frequency-selective channels has two major aspects: Receiver design for MIMO frequency-selective channels and signal design to achieve both spatial diversity by multiple antennas and the frequency diversity by the multipath channel. Since space-time codes are originally designed for flat-fading channels, it is challenging to apply them over frequency-selective channels. One approach is to employ OFDM which converts a frequency-selective channel into parallel independent frequency-flat subchannels using the computationally efficient FFT.

Transmit diversity from orthogonal designs is one of the simplest MIMO techniques. A simple combiner is used at the receiver side to get a full spatial diversity. In next section, we will focus on STBC-OFDM.

4.2.1. Space-Time Block Coded OFDM

Transmitter diversity is an effective technique to combat the fading effect in mobile wireless communications. The STBC technique, one of representative multiple antenna techniques, is most attractive for these purposes since it easily provides the diversity at receiver by transmitting a space-time coded signal through multiple antennas. On the other hand, the OFDM technique has been widely accepted for the transmission of high rate data due to its robustness to inter-symbol interference. In this context, the STBC-OFDM system may be one of the most promising system configurations that can be adopted for the 4th generation mobile systems.

In this section, we will examine the well known Alamouti STBC-OFDM which includes two-transmit antennas and one-receive antenna. A simplified block diagram of the system is shown in Figure 4.2. At time n, a data block $S(n,k)$, $k = 0, 1, 2, ..., K-1$, where K is the number of subcarriers, is coded into two different symbol blocks, $X_i(n,k)$, $i = 1, 2$. After a K-length IFFT operation expressed as follows:

$$x_i(n,m) = \frac{1}{K} \sum_{k=0}^{K-1} X_i(n,k) e^{\frac{j2\pi mk}{K}} \tag{4.4}$$

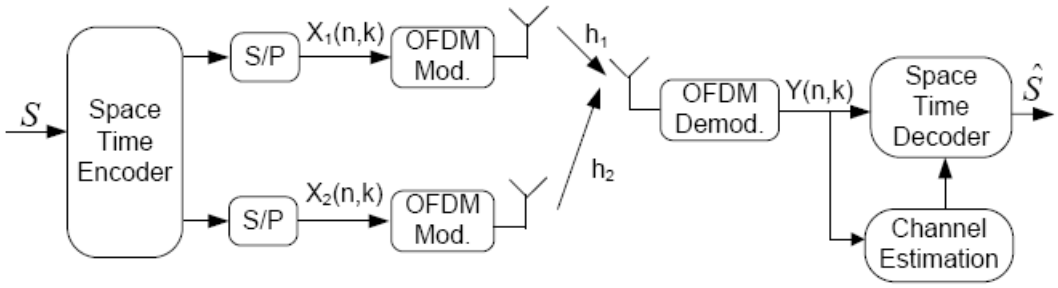

Figure 4.2. Alamouti STBC-OFDM System Model

each block is transmitted through different antennas over the same bandwidth using K OFDM subcarriers. In other words, between each transmit antenna and the receiver there is a communication link established by OFDM.

At time n, $x_1(m)$ and $x_2(m)$, at time $n+1$, $-x_2^*(m)$ and $x_1^*(m)$ are transmitted from antenna one and two, respectively. At the transmitter side, the CP is added to mitigate ISI before IFFT operation because of the property of the OFDM system model as defined in Section 2.2. At the receiver side, firstly this CP is removed and then FFT operation is performed. The received signal is the superposition of the transmitted signals and can be expressed as:

$$Y(n,k) = X_1(n,k)H_1(n,k) + X_2(n,k)H_2(n,k) + N(n,k) \tag{4.5}$$

where $N(n,k)$ is the AWGN with zero mean and σ_N^2 variance and $H_i(n,k)$ denotes the channel frequency response of the multipath channel and the kth subchannel between the ith transmit and receive antenna.

Assuming that the channel is quasi-static and satisfies $H_i(n,k) = H_i(n+1,k) = H_i(k)$, the demodulated signal $Y(n,k)$ is then decoded by the linear maximum-likelihood space-time decoder:

$$\begin{aligned} \tilde{S}(n,k) &= H_1^*(k)Y(n,k) + H_2(k)Y^*(n+1,k) \\ \tilde{S}(n+1,k) &= H_2^*(k)Y(n,k) - H_1(k)Y^*(n+1,k). \end{aligned} \tag{4.6}$$

Finally the estimated symbols $\hat{S}(n,k)$ and $\hat{S}(n+1,k)$ is obtained as defined in Section 2.3.2.1 at Equation (2.34).

4.3. V-BLAST Structured MIMO-OFDM

The V-BLAST structure is a promising method to increase the information capacity of MIMO systems by transmitting parallel data streams from multiple antennas and applying interference cancellation techniques at the receiver. OFDM is a robust system in frequency-selective fading channels. Hence, the combination of V-BLAST and OFDM is one of the strong candidate for the future wireless communication systems. A simple block diagram of the V-BLAST structured MIMO-OFDM is shown in Figure 4.3. The

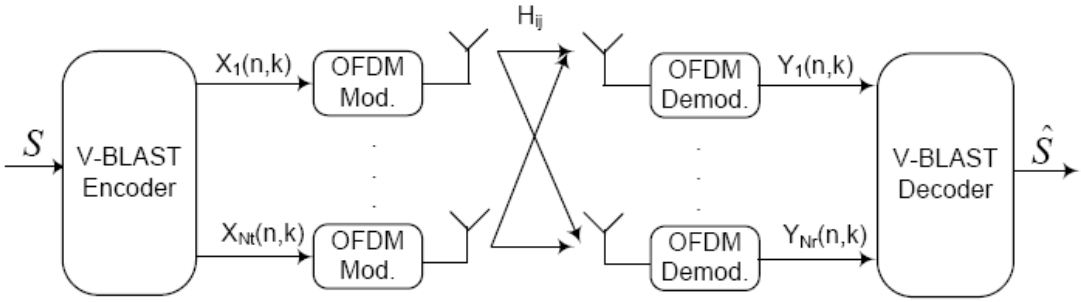

Figure 4.3. V-BLAST OFDM System Model

serial transmit symbols are first paralled to N_t data streams with a V-BLAST encoder. Then, these datas are OFDM modulated as defined in Section 2.2 and transmitted from N_t transmit antennas simultaneously. The spectrum is used efficiently when compared to SISO systems, because many data streams are sent on the same subcarrier. The capacity of the system increases linearly with the number of transmit antennas. At the receiver, the signals from N_t transmit antennas are superimposed and the output of FFT at the jth receive antenna can be expressed as given in Equation (4.1).

At the receiver, the V-BLAST structure is used as an interference cancellation technique to detect the different data streams from the superimposed signal as defined in Section 2.3.1.1.

4.4. Channel Estimation for MIMO-OFDM

In a MIMO-OFDM system, the receiver should know the frequency response of the spectral and spatial channels between the transmit and receive antennas to achieve the coherent signal detection. The problem of channel estimation for OFDM has been well

researched; however, the results are not directly applicable to MIMO-OFDM systems. In MIMO systems, the number of channels increases by a factor of $N_t N_r$. This significantly increases the number of unknowns to be solved. Conventional estimation techniques for SISO systems have to be modified to be applicable in MIMO systems.

4.4.1. Pilot-Based Channel Estimation for MIMO-OFDM Systems

Pilot-based channel estimation techniques for single transmit antenna have been defined in Section 3.1.1. The channel estimation with pilot symbols is performed easily by using a simple LS algorithm for SISO-OFDM systems. However, it is not easy for MIMO-OFDM systems to estimate the channel, since the received signal is the superposition of the transmitted signals. Different pilot structures are proposed to make the channel estimation issue easier for MIMO-OFDM systems. In one study, to estimate the channel from the ith transmit antenna to the receive antenna, the pilot symbols are sent from only the ith transmit antenna, while the other antennas either transmit null symbols or stop transmission (Alamouti 1998). In this technique, N_t times as many pilot symbols are needed to estimate all the channels in an N_t transmit antennas system as compared to that required for a single antenna system. This technique is spectrally ineffiecient because of the expansion in pilot symbols. Thus, a more efficient technique was proposed by Lee and Williams in (Lee and Williams 2001, 2002). As seen in Figure 4.4 for two-transmit antennas system, they transmitted pilot symbols from different transmitters that occupy different frequency subcarriers. Thus, the received signal contains data from only one transmitter and the channel over which the pilot subcarriers of this transmitter are sent, can be estimated with a simple LS algorithm defined in Section 3.1.1.1. The received signal is simply expressed in a general form for two-transmit and one-receive antenna system as:

$$Y(n) = H_1(n)X_1(n) + H_2(n)X_2(n) + N(n) \tag{4.7}$$

where n is the time index.

According to this pilot arrangement, at time n, we know that either $X_1(n)$ or $X_2(n)$ is pilot symbol and other is null symbol at the same subcarrier. Therefore, the channel estimation is not difficult in this situation. The channel belongs to pilot symbols

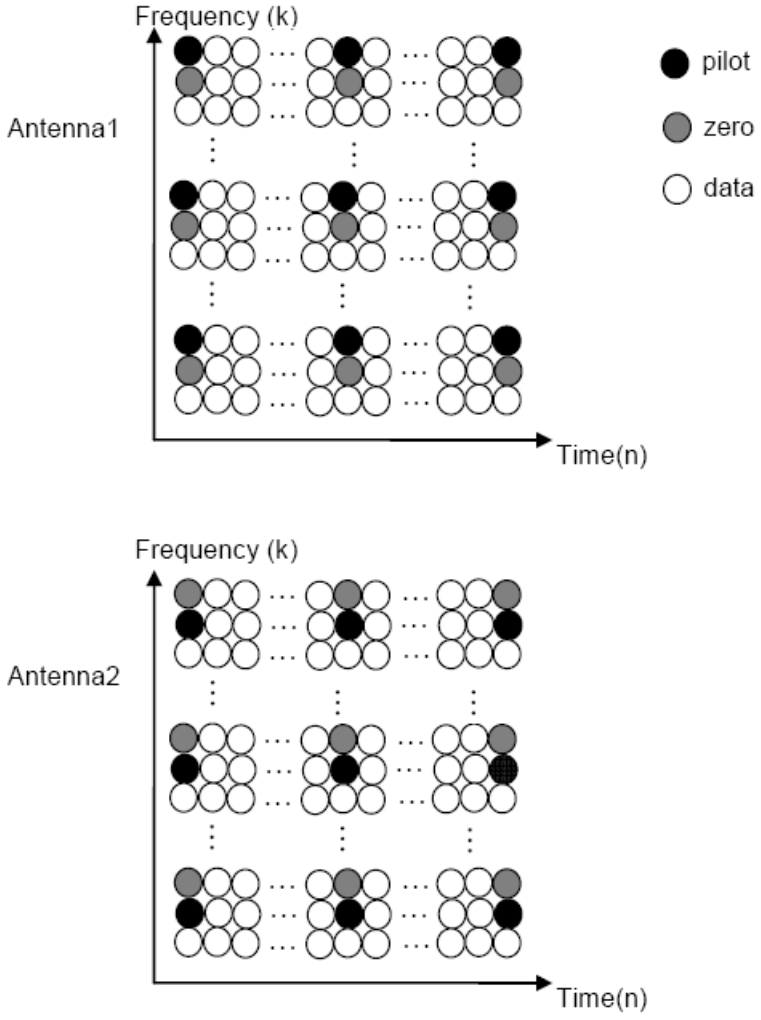

Figure 4.4. Pilot Symbol Pattern for an example OFDM transmitter diversity $N_t = 2$

can be estimated using a simple LS algorithm as:

$$\hat{H}_i(n) = \frac{Y(n)}{X_i(n)}. \tag{4.8}$$

Then an interpolation technique is used to estimate all channel coefficients.

The channel also can be estimated by transmitting pilot symbols from different transmitters at the same frequency bin simultaneously. So, the received signal at the pilot positions will be the superposition of the signals that come from different transmit antennas. However, it is really a difficult problem to solve. One of the techniques proposed to solve this problem is sending the pilot symbols using Space-Time Block Codes (Guo et al. 2003). The pilot placement structure can be seen in Figure 4.5. To understand this technique well, we can study on specific examples. Firstly, the channel estimation process for two-transmit and one-receive antennas is studied. We will derive our equations for the pilot symbols. The received signal model for this system can be expressed in matrix form as:

$$\begin{bmatrix} Y_1(k_p, n) \\ Y_2(k_p, n+1) \end{bmatrix} = \begin{bmatrix} X_1(k_p, n) & X_2(k_p, n) \\ -X_2(k_p, n+1)^* & X_1(k_p, n+1)^* \end{bmatrix} \begin{bmatrix} H_1(k_p) \\ H_2(k_p) \end{bmatrix} + \begin{bmatrix} N_1(k_p, n) \\ N_2(k_p, n+1) \end{bmatrix} \tag{4.9}$$

where k_p is the subcarrier index represents the pilot positions, $Y_1(k_p, n)$ and $Y_2(k_p, n+1)$ are the received signals at time n and $n+1$, respectively. The STBC-OFDM system assumes that the channel frequency response is identical between the N_t consecutive symbol intervals. That is, it assumes that $H_i(k_p, n) = H_i(k_p, n+1) = H_i(k_p)$, $i = 1, 2$. In this case, at the nth symbol interval, from the first antenna $X_1(k_p, n)$ is transmitted, and from the second antenna $X_2(k_p, n)$ is transmitted. During the next symbol interval, the first antenna sends $-X_2(k_p, n+1)^*$ and the second antenna sends $X_1(k_p, n+1)^*$. We can also write the equations of the system by omitting the pilot subcarrier index k_p and time index n in order to simplfy as;

$$\begin{aligned} Y_1 &= X_1 H_1 + X_2 H_2 + N_1 \\ Y_2 &= -X_2^* H_1 + X_1^* H_2 + N_2. \end{aligned} \tag{4.10}$$

The estimated channel frequency responses can be found by using the two equations given in Equation (4.10). The estimation results;

$$\hat{H_1} = \frac{Y_1 X_1^* - Y_2 X_2}{2} \quad , \quad \hat{H_2} = \frac{Y_1 X_2^* + Y_2 X_1}{2}. \tag{4.11}$$

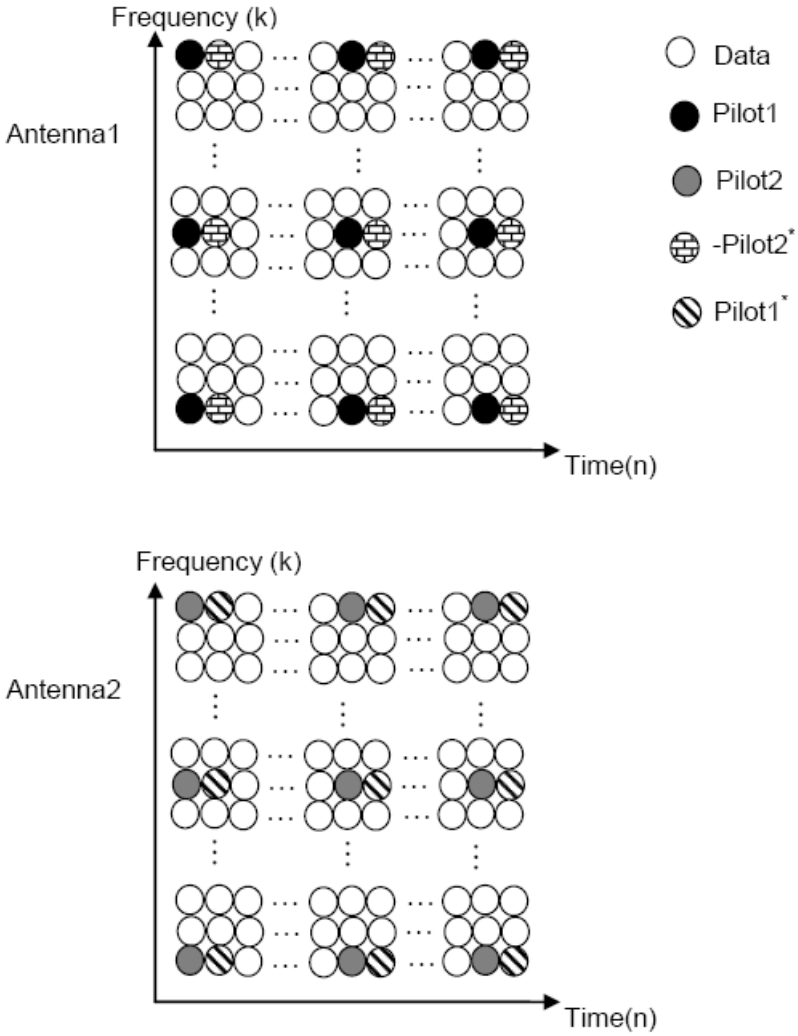

Figure 4.5. Superimposed Pilot Symbol Pattern for OFDM transmitter diversity $N_t = 2$

This technique is also applied to a system which contains two-transmit and two-receive antennas. For this system, the number of the channels which will be estimated will be increased. The system is expressed in matrix form as:

$$\begin{bmatrix} Y_1(k_p) & Y_2(k_p) \\ Y_3(k_p) & Y_4(k_p) \end{bmatrix} = \begin{bmatrix} X_1(k_p) & X_2(k_p) \\ -X_2(k_p)^* & X_1(k_p)^* \end{bmatrix} \begin{bmatrix} H_{11}(k_p) & H_{12}(k_p) \\ H_{21}(k_p) & H_{22}(k_p) \end{bmatrix} + \begin{bmatrix} N_{11}(k_p) & N_{12}(k_p) \\ N_{21}(k_p) & N_{22}(k_p) \end{bmatrix} \tag{4.12}$$

This matrix form can also be written in equation form by omitting the k_p for the simplicity as:

Time n

$$\begin{aligned} Y_1 &= X_1 H_{11} + X_2 H_{21} + N_{11} \\ Y_2 &= X_1 H_{12} + X_2 H_{22} + N_{12} \end{aligned} \tag{4.13}$$

Time $n+1$

$$\begin{aligned} Y_3 &= -X_2^* H_{11} + X_1^* H_{21} + N_{21} \\ Y_4 &= -X_2^* H_{12} + X_1^* H_{22} + N_{22} \end{aligned} \tag{4.14}$$

Using the Equations (4.13) and (4.14) the channel estimates are found as;

$$\begin{aligned} \hat{H}_{11} &= \frac{X_1^* Y_1 - X_2 Y_3}{2} \\ \hat{H}_{21} &= \frac{X_2^* Y_1 + X_1 Y_3}{2} \\ \hat{H}_{12} &= \frac{X_1^* Y_2 - X_2 Y_4}{2} \\ \hat{H}_{22} &= \frac{X_2^* Y_2 + X_1 Y_4}{2} \end{aligned} \tag{4.15}$$

These pilot-based channel estimation techniques for MIMO-OFDM systems are compared in terms of BER and MSE. The BER performance comparison of zero added technique and superimposed pilot technique is shown in Figure 4.6 and the channel estimation performance comparison is shown in Figure 4.7. Using these results, it is obviously seen that the performance of the superimposed signal is better than zero added pilot structure. Zero added pilot structure is spectrally inefficient because many null symbols are transmitted instead of the data symbols from different transmit antennas. There is a

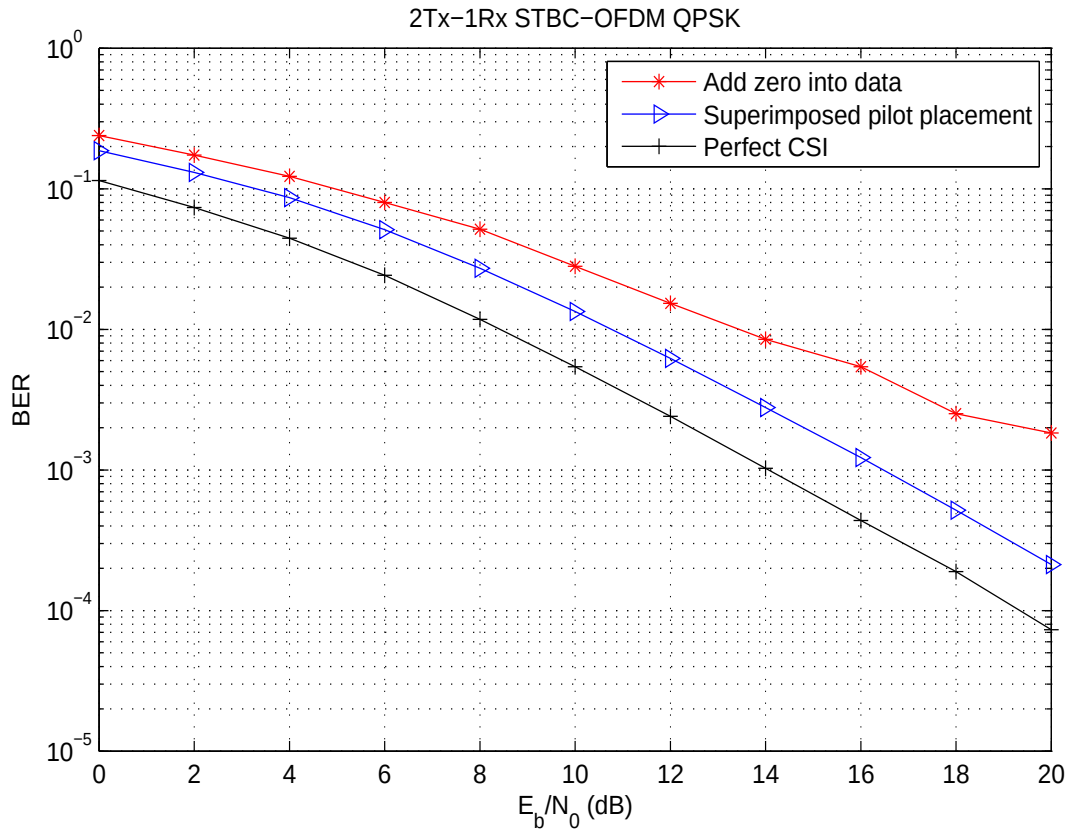

Figure 4.6. BER performance of the pilot-based channel estimation for STBC-OFDM

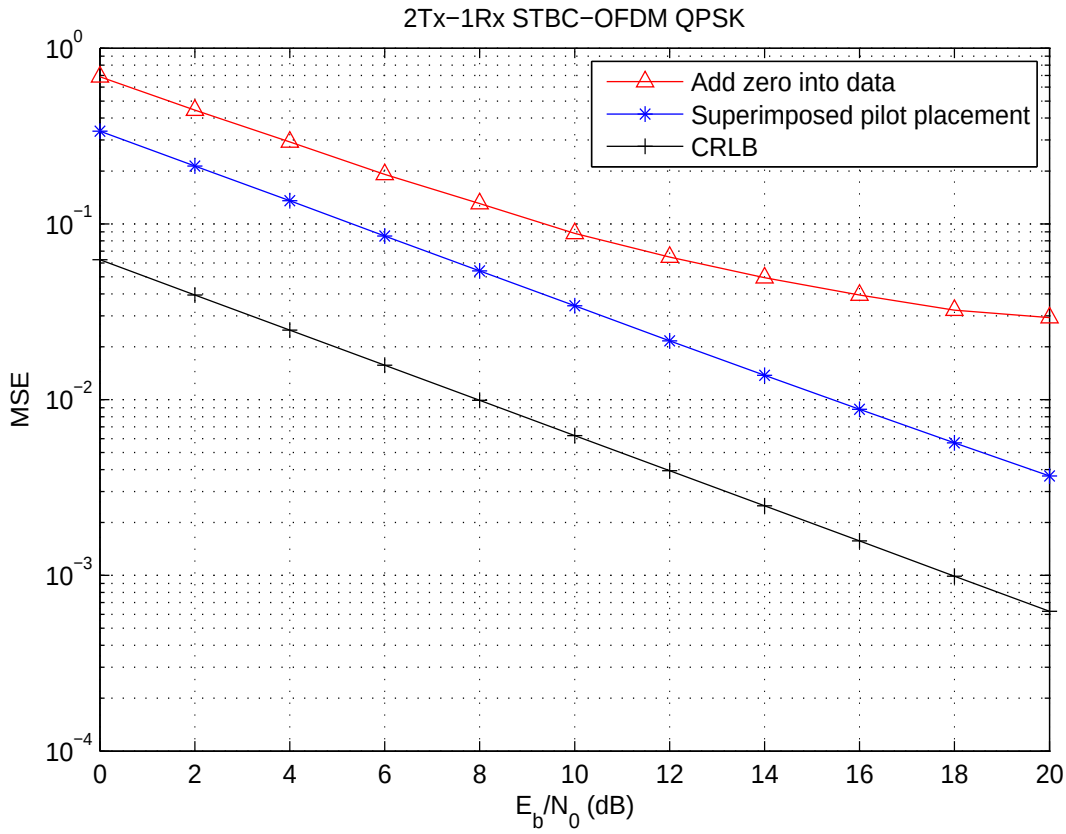

Figure 4.7. MSE performance of the pilot-based channel estimation for STBC-OFDM

trade off between the complexity and performance for both techniques. The zero added technique has lower computational complexity but poor BER performance. Thus, it is a proper choice to use superimposed pilot structure.

4.5. EM-Based Joint Channel Estimation and Signal Detection for V-BLAST MIMO-OFDM Systems

The channel estimation and signal detection processes for V-BLAST OFDM systems can be performed jointly. It is known that the signal detection of V-BLAST structured MIMO-OFDM uses linearly integrated nulling and symbol cancellation on each subcarrier to successively compute the signal from each transmit antenna as defined in Section 2.3.1.1. The general idea for V-BLAST OFDM detection process is to detect the strong signal, remove its effect from the whole received signal and detect the other weak signals. From this definition, it can be thought that if the signal from ith transmit antenna to the jth receive antenna is strong this means, the channel between them is estimated accurately. We also consider the channel estimation is not performed well for the weak signals. Thus, how to improve the channel estimation performance of the weak signals is the problem for us. This problem can be solved by using joint signal detection and channel estimation (Song et al. 2005). First of all, the initial channel estimation $\mathbf{H}_{init}$ is found by using pilot symbols as given in Section 4.4.1. The V-BLAST signal detections for different subcarriers are independent. Thus the initial channel estimation matrix for the kth tone $\mathbf{H}_k$, can be expressed as:

$$\mathbf{H}_k = \begin{bmatrix} H_{11}(n,k) & \dots & H_{1N_r}(n,k) \\ \vdots & \ddots & \vdots \\ H_{N_t1}(n,k) & \dots & H_{N_tN_r}(n,k) \end{bmatrix} \tag{4.16}$$

where n is the time index, N_t and N_r gives the number of transmit and receive antennas respectively.

Then the steps for the joint channel estimation and detection method can be given as below:

For kth tone and each OFDM symbol independently:

$\mathbf{H}_k = \mathbf{H}_{init}$;

$d = 1, ..., D$;

{

$i = 1, ..., N_t$;

{

$$\mathbf{G}_k = (\mathbf{H}_k^H \mathbf{H}_k)^{-1} \mathbf{H}_k^H;$$

$$lyr = \arg\min_{j \neq d} \|(\mathbf{G}_k)_j\|^2;$$

$$\mathbf{w}_{lyr} = (\mathbf{G}_k)_{lyr};$$

$$\tilde{Y}_{lyr}(n,k) = \mathbf{w}_{lyr} \mathbf{Y}^i(n,k);$$

$$\hat{b}_{lyr} = Q(\tilde{Y}_{lyr}(n,k));$$

$$\mathbf{Y}^{i+1}(n,k) = \mathbf{Y}^i(n,k) - \hat{b}_{lyr}(\mathbf{H}_k)_{lyr};$$

$$(\mathbf{H}_k)_{lyr} = 0;$$

}

$(\mathbf{H}_k)_d = Channelupdate(\mathbf{Y}^{N_t}(n,k), \mathbf{H}_k)$;

}

where $Channelupdate$ function updates the worst channel in the system using EM algorithm defined in Section 3.1.2.2.

If we define this process expressed above in detail, the first step is the computation of the nulling vector to perform interference cancellation. The nulling matrix $\mathbf{G}_k$ is found by using the initial estimation $\mathbf{H}_k$. For signal from each transmit antenna, which is called *layer*, the nulling vector is the corresponding row of the nulling matrix $\mathbf{G}_k$. Using the nulling matrix and nulling vectors, the lyrth layer, which is strong, is extracted from the system.

$$\tilde{Y}_{lyr}(n,k) = (\mathbf{G}_k)_{lyr} \mathbf{Y}^i(n,k) \tag{4.17}$$

where $\mathbf{Y}^i(n,k) = [Y_1(n,k), Y_2(n,k), ..., Y_{N_r}(n,k)]^T$ is the received signal vector for the kth subcarrier. The decoded lyrth layer is substracted from the total received signal, after

hard decision of the extracted signal $\tilde{Y}_{lyr}(n,k)$.

$$\mathbf{Y}^{i+1}(n,k) = \mathbf{Y}^{i}(n,k) - \hat{b}_{lyr}(\mathbf{H}_k)_{lyr} \tag{4.18}$$

where $\hat{b}_{lyr}$ is hard decison symbols and $(\mathbf{H}_k)_{lyr}$ is the lyrth column of the channel information matrix $\mathbf{H}_k$.

After the lyrth layer is detected and cancelled, the lyrth column of $\mathbf{H}_k$ is set to zero. After detecting the strong layer, we do not continue to detect the signals. Instead of the detection algorithm we update the channel belonging to the weak signals with $Channelupdate$ function defined above. When the channel is updated, the detection algorithm starts from the beginning. The whole process is a process of iteration. After D loops of outer iterations, the iteration steps into converge and all the layers of the V-BLAST signals are detected finally.

4.6. Simulation Results

In this section, the computer simulations are given to demonstrate the BER and MSE performances of the systems defined above. The simulation results are grouped for STBC-OFDM and V-BLAST structured OFDM.

4.6.1. STBC-OFDM Simulation Results

The system used for the simulation is built with two-tranmit antennas and one-receive antenna. The BER and MSE performances, which belongs to the combination of the STBC and OFDM, are compared. The parameters used in our simulation are given in Table 4.1.

The estimation process started by finding an initial channel estimation with pilot symbols. The pilot symbols are distributed in the frequency-time lattices as seen in Figure 4.5. The channel is estimated as defined in Section 4.4.1. Then, the EM algorithm is applied to improve the channel estimation performance as expressed in Section 3.1.2.2. The observed data $(\mathbf{Y})$ is decomposed into two components and complete data $(\mathbf{Z}_1, \mathbf{Z}_2)$ is obtained as;

$$\mathbf{Z}_i = \mathbf{X}_i\mathbf{H}_i + \mathbf{N}_i, \qquad i = 1,2 \tag{4.19}$$

where $\mathbf{N}_i, i = 1, 2$ are obtained by arbitrarily decomposing the total noise $\mathbf{N}$ into two components such that $\mathbf{N}_1 + \mathbf{N}_2 = \mathbf{N}$. $\mathbf{N}_1$ and $\mathbf{N}_2$ are designed as the half of the total noise $\mathbf{N}$. Thus the relationship between the complete data $(\mathbf{Z}_1, \mathbf{Z}_2)$ and incomplete data $(\mathbf{Y})$ is given by $\mathbf{Y} = \mathbf{Z}_1 + \mathbf{Z}_2$.

Table 4.1. Simulation parameters for STBC-OFDM

Bandwith of the system	$800kHz$
Number of subcarriers	64
Number of CP	16
Number of OFDM symbols in a frame	64
Number of pilot symbols in a frame	64
Number of data symbols in a frame	4032
Symbol duration (T_{OFDM})	$80\mu s$
CP duration (T_{CP})	$20\mu s$
Total OFDM symbol duration $(T_{OFDM+CP})$	$100\mu s$
Maximum Doppler frequency (f_{dmax})	$100Hz$
Modulation type	$QPSK$

In Figure 4.8, the BER performance and in Figure 4.9 the MSE performance of the QPSK modulated STBC-OFDM (2Tx-1Rx) system is given. According to these figures, we observe that the EM-based channel estimation algorithm can improve the BER and MSE. Moreover, it can achieve a BER performance close to the case where the channel characteristic is completely known at the receiver in high SNR region. However, there is still BER gap between the lower bound and the BER of the EM-based algorithm. The MSE is also very close to the CRLB when the SNR increases.

It is well known that there is a tradeoff between the number of the pilot symbols and the system performance. We can improve the system performance by sending many pilot symbols in an OFDM frame. However, our aim is to use the bandwidth efficiently. Thus, we studied on a method called sequential channel estimation. This method is also studied for SISO-OFDM system in (Baştürk and Özbek 2007) and simulation results were given in Section 3.1.4.1. According to this method, the pilot symbols are placed into the first and second OFDM symbols as seen in Figure 4.10 and an initial channel estimation is

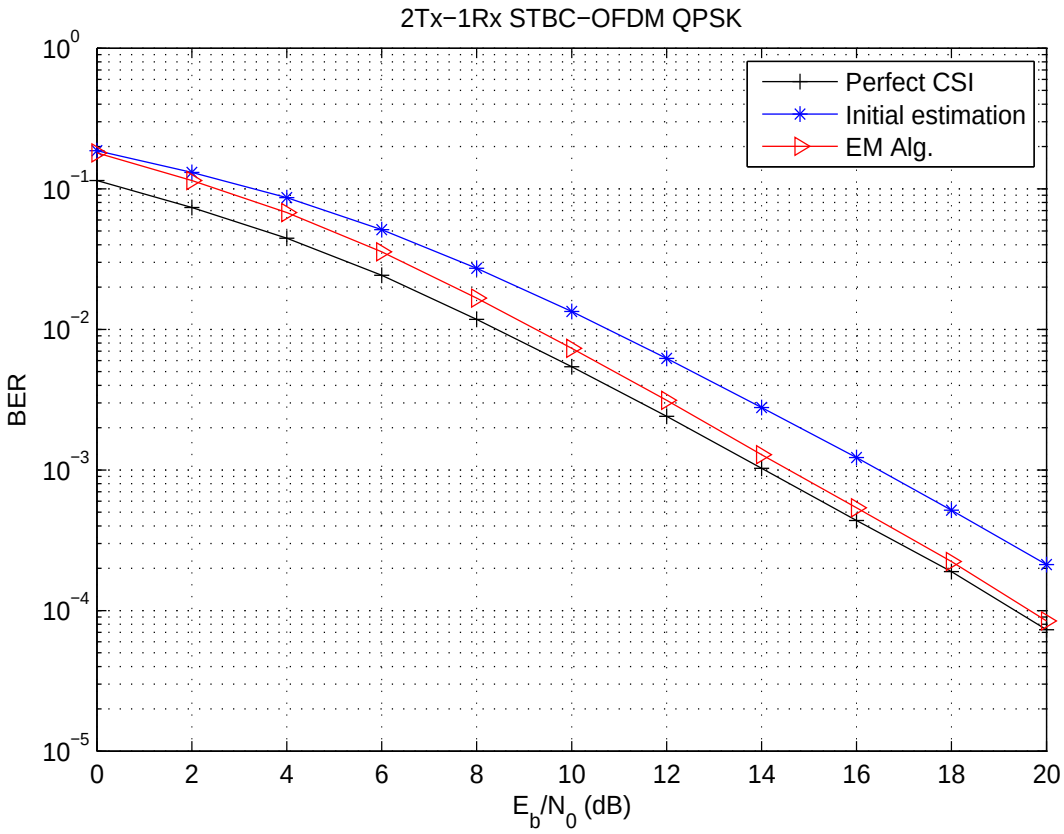

Figure 4.8. BER performance of the STBC-OFDM

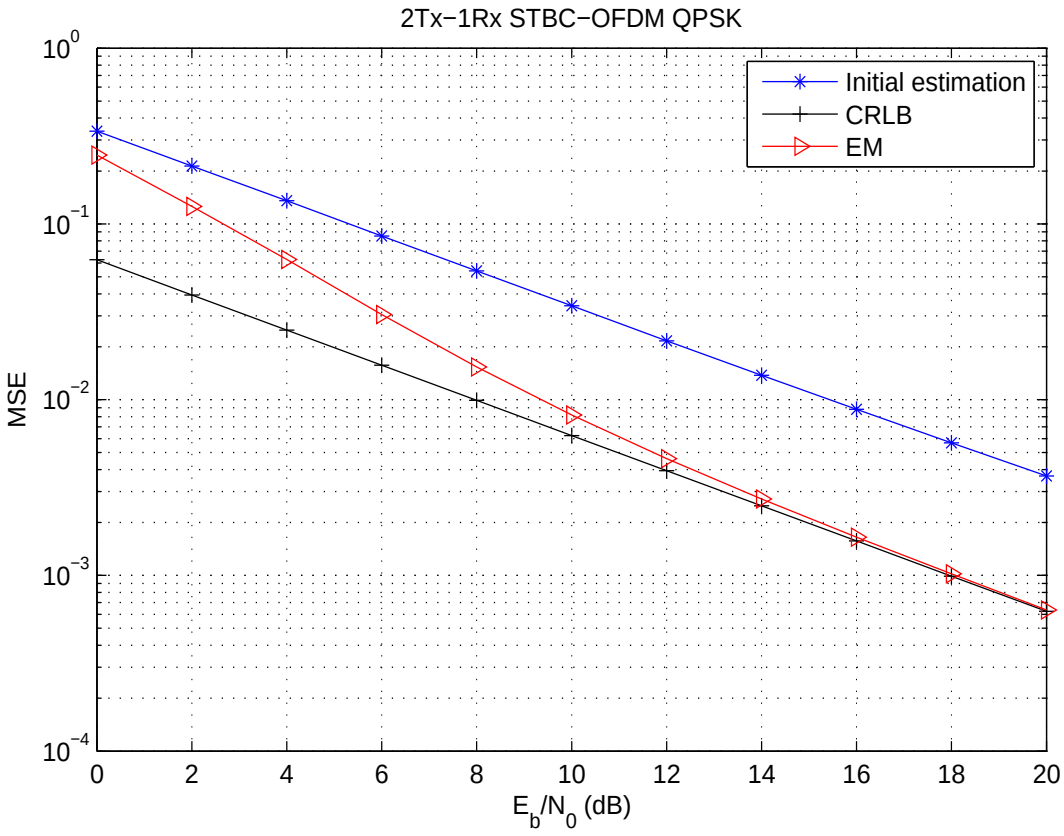

Figure 4.9. MSE performance of the STBC-OFDM

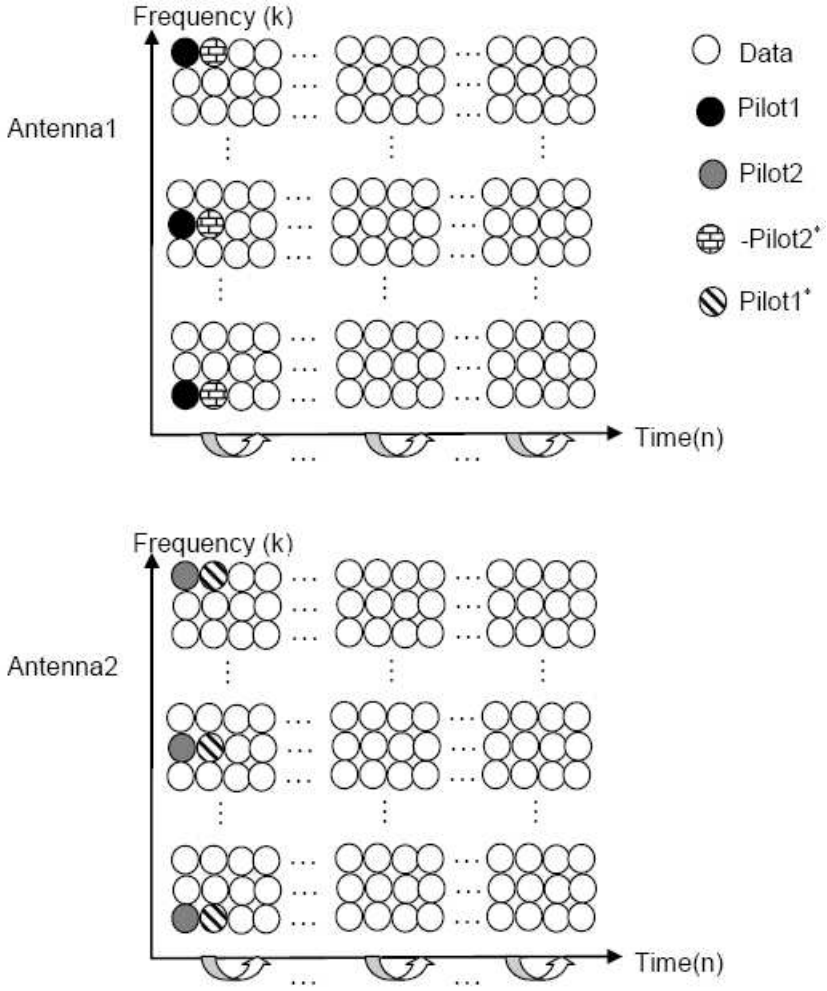

Figure 4.10. Pilot arrangement for STBC-OFDM sequential channel estimation

performed. The channel coefficients at pilot positions are found by LS algorithm and then DFT-based interpolation is used to estimate all channel coefficients. These estimates are used as the initial estimation of the next OFDM symbol and the EM algorithm is applied to improve the estimation accuracy. This process is repeated until all channel coefficients are estimated in a frame.

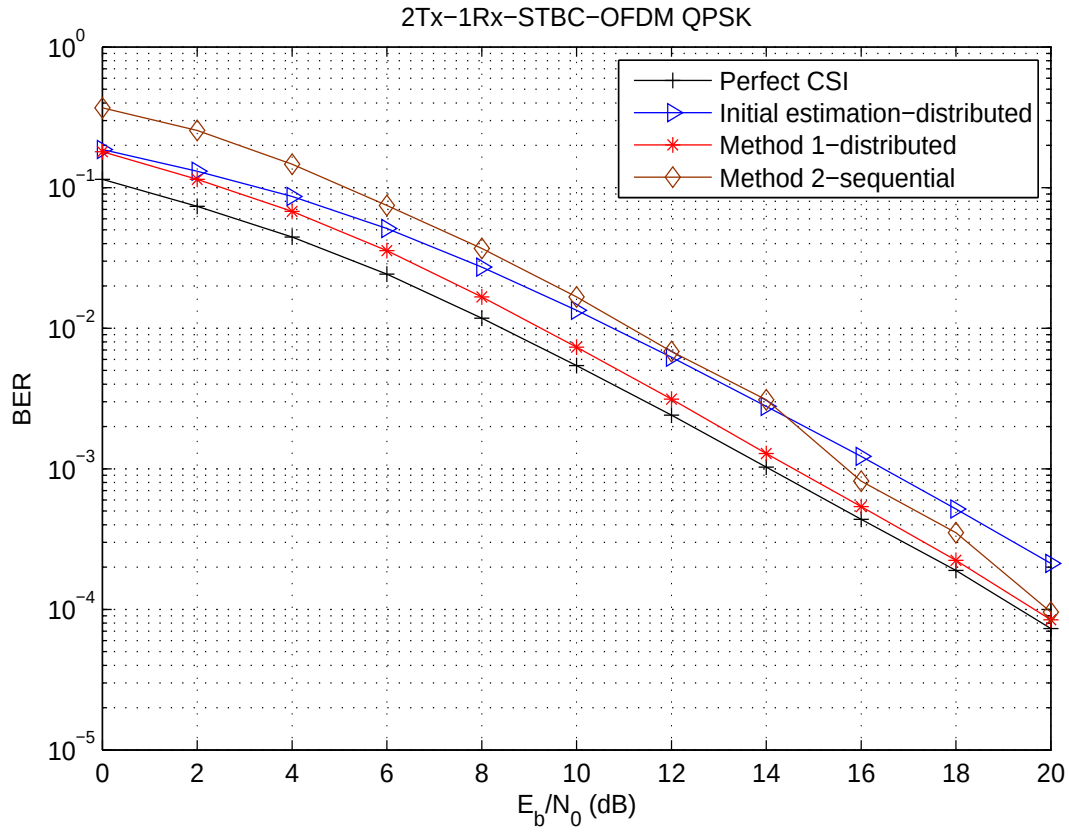

Figure 4.11. Different pilot arrangement BER comparison for STBC-OFDM

In this method, 8 pilot symbols and 4088 data symbols are used in an OFDM frame. The distance between two pilot symbols in the frequency domain $D_f = 8$. Other simulation parameters are the same as given in Table 4.1. For simplicity, we denoted this method as Method 2 and the first method, which uses the distributed pilot symbols in the frequency-time lattices (Figure 4.5), is called as Method 1. We compared the performance of the two methods in terms of BER and MSE.

In Figure 4.11, the BER performances are given for the two methods. The performance of Method 2 is worse than others in low SNR values. However, the performance of the Method 2 is better than initial channel estimation for E_b/N_0 >14 dB and its performance is getting closer to the performance of Method 1. When E_b/N_0 =20 dB their

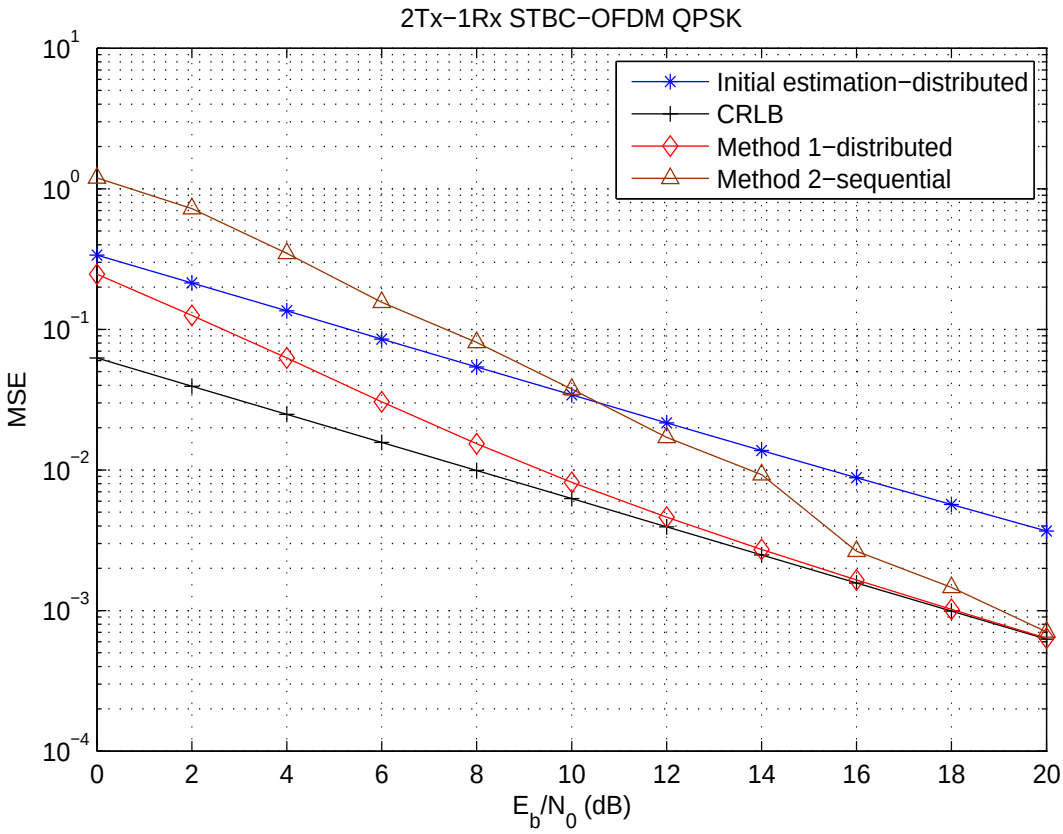

Figure 4.12. Different pilot arrangement MSE comparison for STBC-OFDM

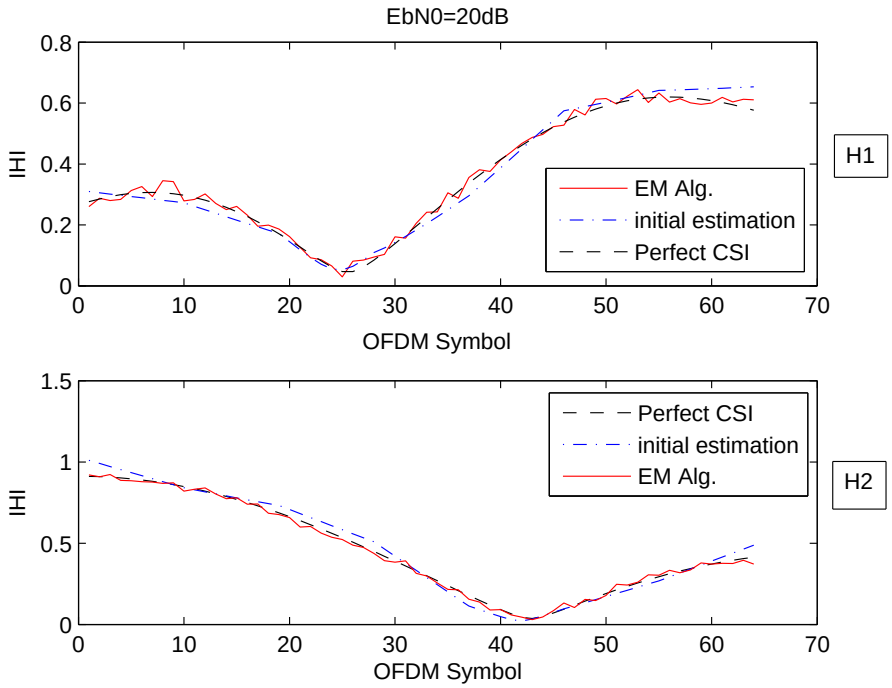

Figure 4.13. Tracking the channel variations of Method 1 in time for STBC-OFDM

performances are the same.

Figure 4.12 compares the MSE performance of the two methods. It is seen that the Method 2 is better than the initial channel estimation after 14 dB. Method 2 is also getting closer to Method 1 and CRLB for high SNR values.

We can conclude that Method 2 is suitable to use for high SNR values such as above 16dB. It has lower number of pilot symbols and only need to perform frequency domain interpolation, thus, it is spectrally efficient and less complex than Method 1 as seen from Table 4.2.

Table 4.2. Comparison of Method 1 and Method 2 for STBC-OFDM

	Method 1(Distributed)	Method 2(Sequential)
Number of pilot symbols in a frame	64	8
Frequency axes interpolation	DFT-based	DFT-based
Time axes interpolation	Linear interpolation	No interpolation
Normalized simulation duration for one OFDM frame	1	0.67

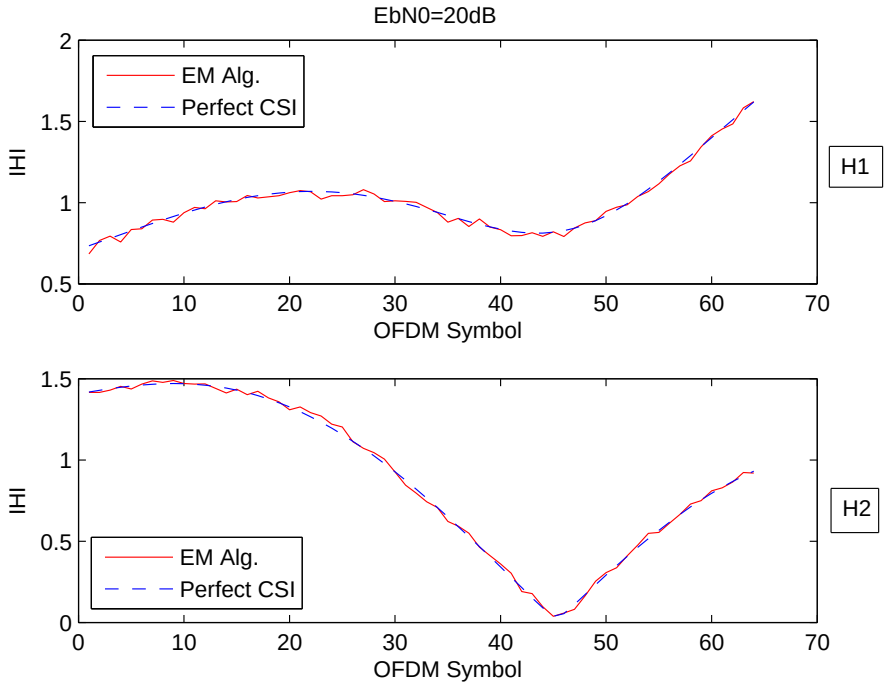

Figure 4.14. Tracking the channel variations of Method 2 in time for STBC-OFDM

Finally, we obtained the Figures 4.13 and 4.14 in order to show how Method 1 and Method 2 are tracking the channel variations. For both methods, it is obviously seen that especially EM-based channel estimation tracks the channel variations very well.

4.6.2. V-BLAST OFDM Simulation Results

The V-BLAST OFDM structure was defined in Section 4.3. In this part, the simulation results will be given for two-transmit and two-receive antennas system. The simulation parameters used in the simulation is given in Table 4.1.

In this simulation, again pilot symbols are used for the initial channel estimation. The pilot symbols are space-time block coded to estimate the channel easily. The channel frequency responses at the pilot positions found by using Equation (4.15). Then interpolation techniques in the time and frequency axes are used to estimate all channel coefficients in an OFDM frame. The EM algorithm is applied to all channel estimates to increase the channel estimation accuracy as defined in Section 3.1.3.2. Also, to decompose the superimposed noise component at the receiver, the same design, which is expressed in Section 4.6.1 is utilized.

Figure 4.15 compares the BER performances of the V-BLAST OFDM system. It is seen that the EM algorithm improves the BER performance. It is almost the same with perfect CSI for high SNR values.

In Figure 4.16, the MSE performance of the system is shown. The EM-based channel estimation is getting closer to CRLB when E_b/N_0 >14 dB. There is really a big gap between the pilot-based initial estimation and the EM-based channel estimation.From these figures, we see that EM algorithm improves the channel estimation performance.

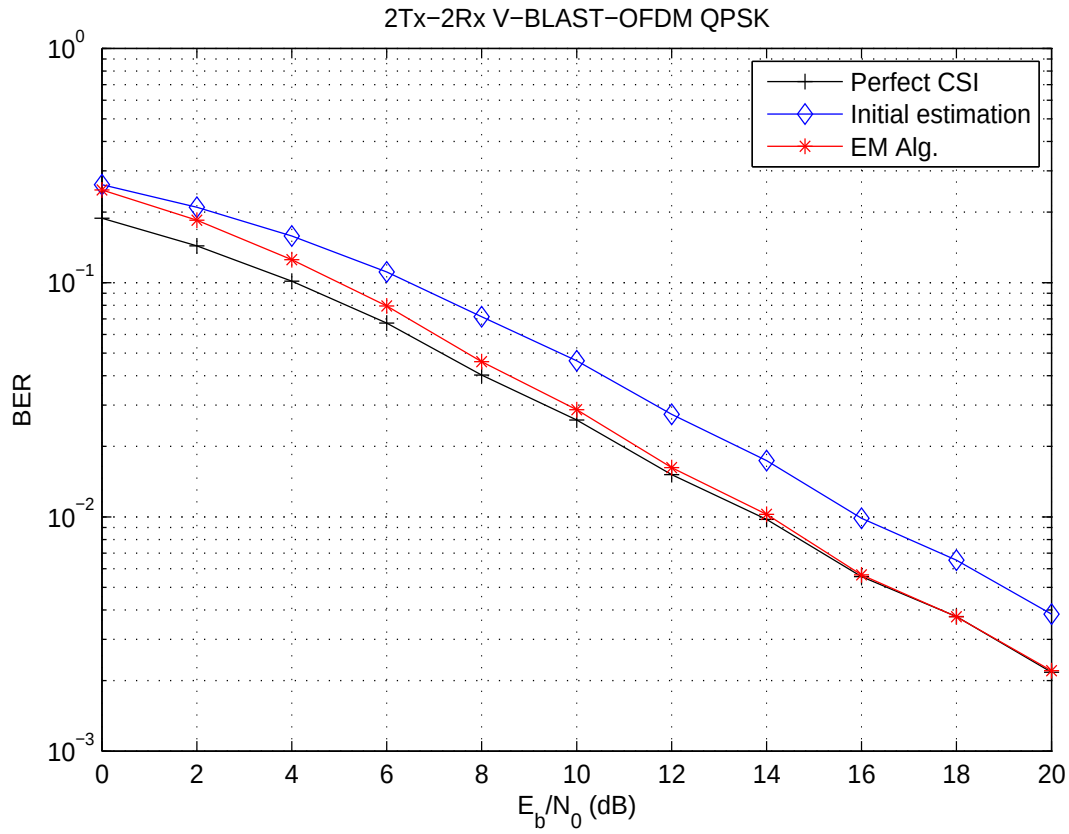

Figure 4.15. BER for the V-BLAST structured MIMO-OFDM

After comparing the pilot and EM-based channel estimation for V-BLAST MIMO-OFDM systems, we compared two methods which we called as Method 1 and Method 2. We arranged the pilot symbols as shown in Figure 4.5 for Method 1 and Figure 4.10 for Method 2. We performed the same processes as told in Section 3.1.4. Figure 4.17 shows the BER comparison of two methods and we can see above 10 dB Method 2 is getting closer to Method 1 and perfect CSI. From Figure 4.18, we can again say that the channel estimation performance of Method 2 is better above 10 dB. Method 2, which we named as sequential channel estimation is suitable when E_b/N_0 >10 dB and it has

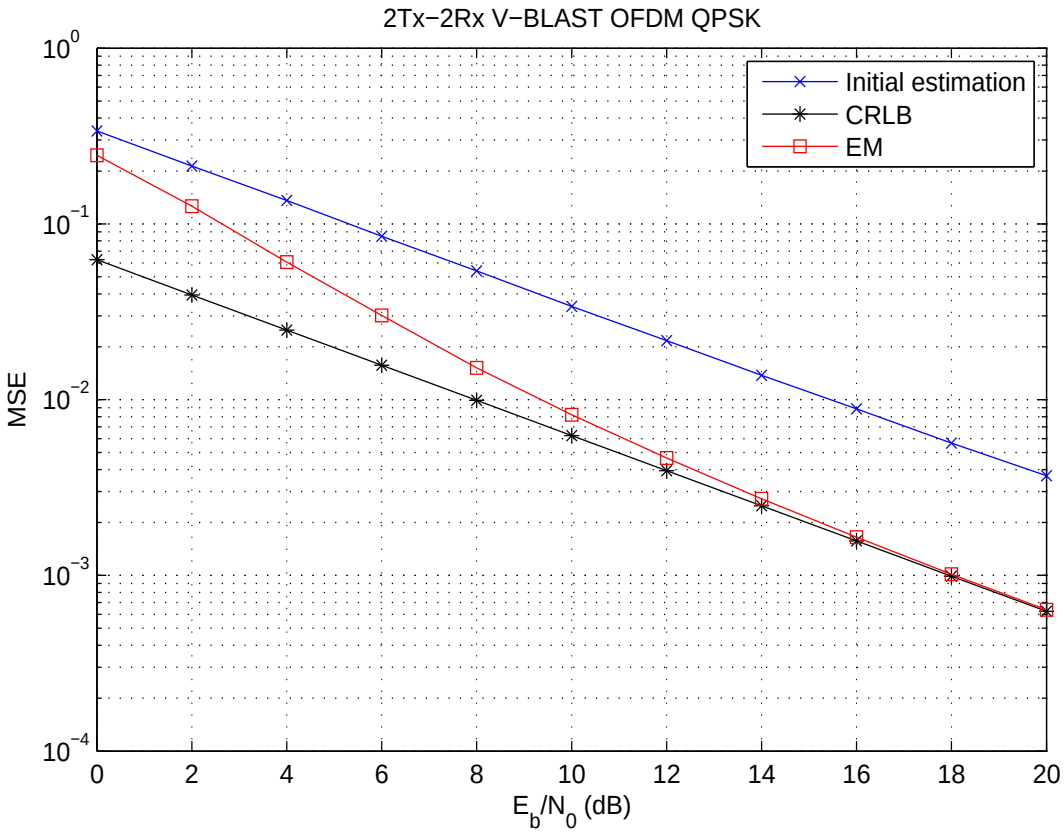

Figure 4.16. MSE for the V-BLAST structured MIMO-OFDM

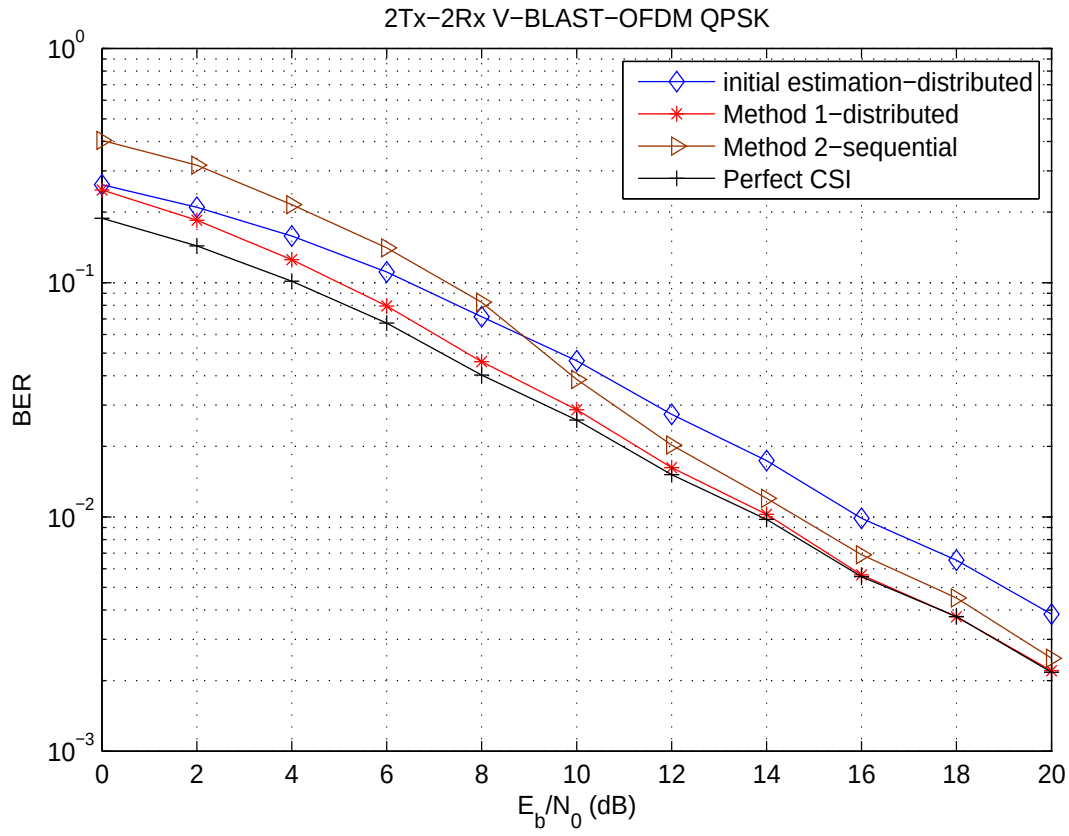

Figure 4.17. Comparison of BER of two methods for the V-BLAST MIMO-OFDM

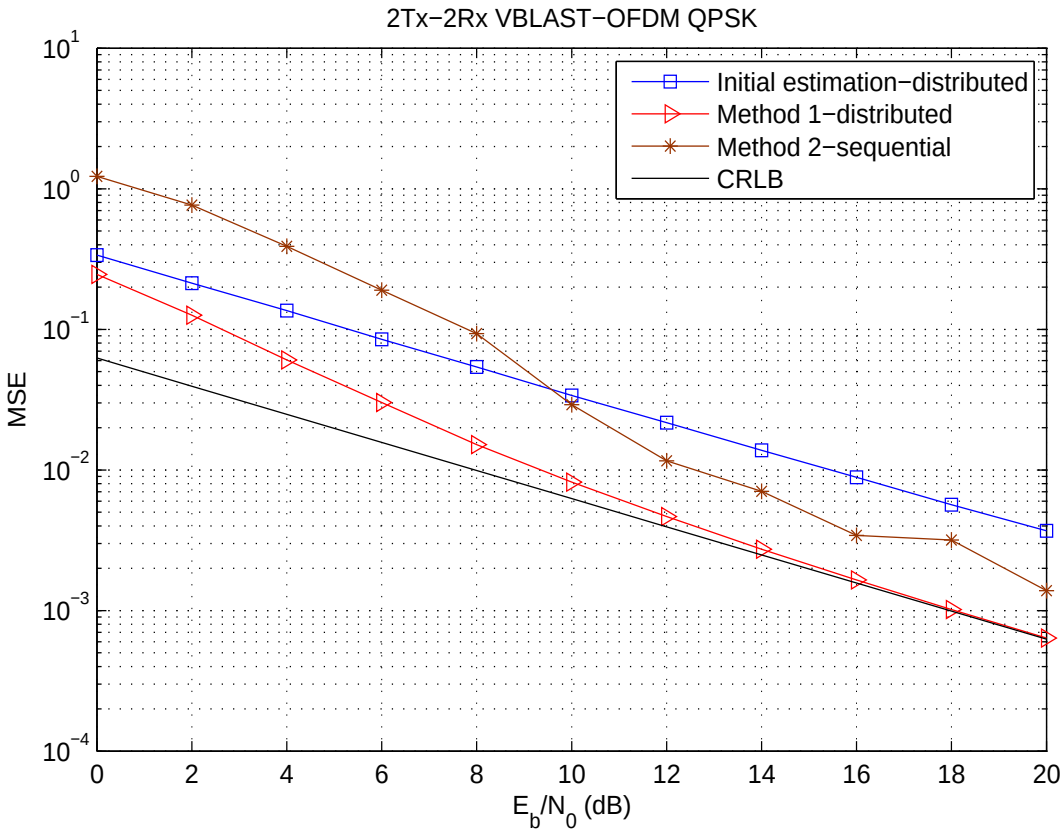

Figure 4.18. Comparison of MSE of two methods for the V-BLAST MIMO-OFDM

some advantages when compared to Method 1 as shown in Table 4.3. Method 2 uses the spectrum efficiently with lower computational complexity.

Table 4.3. Comparison of Method 1 and Method 2 for V-BLAST MIMO-OFDM

	Method 1(Distributed)	Method 2(Sequential)
Number of pilot symbols in a frame	64	8
Frequency axes interpolation	DFT-based	DFT-based
Time axes interpolation	Linear interpolation	No interpolation
Normalized simulation duration for one OFDM frame	1	0.5

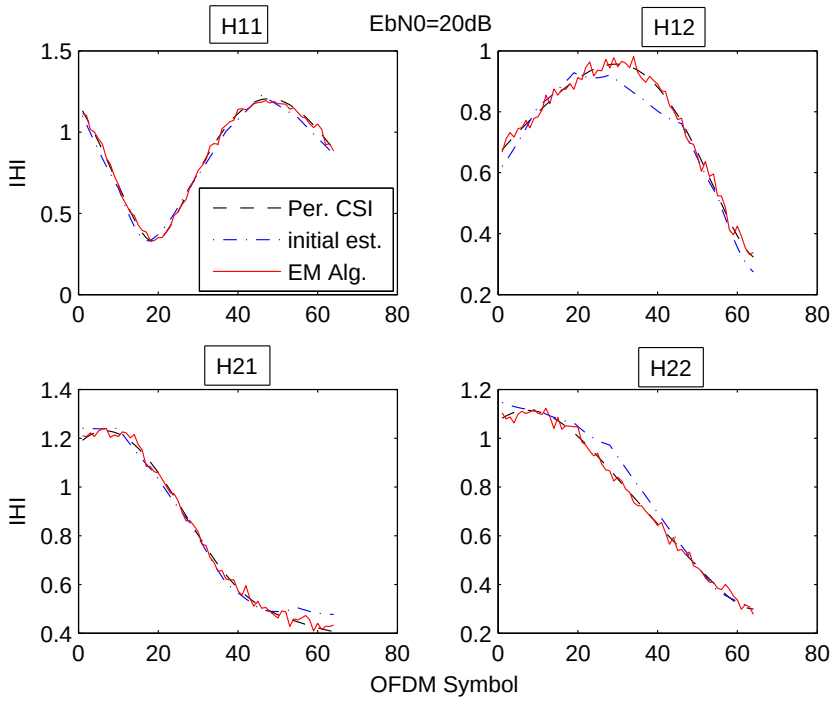

Figure 4.19. Tracking the channel variations of Method 1 in time for V-BLAST OFDM

We also obtained the channel tracking graphics of two methods. From Figure 4.19, we can see that the four channels are being tracked well for Method 1. Figure 4.20 shows us the sequential channel estimation method is also tracking the channel variations in time very well.

Moreover, the BER and MSE results are obtained for joint channel estimation and signal detection as defined in Section 4.5. The simulation parameters given in Table 4.1

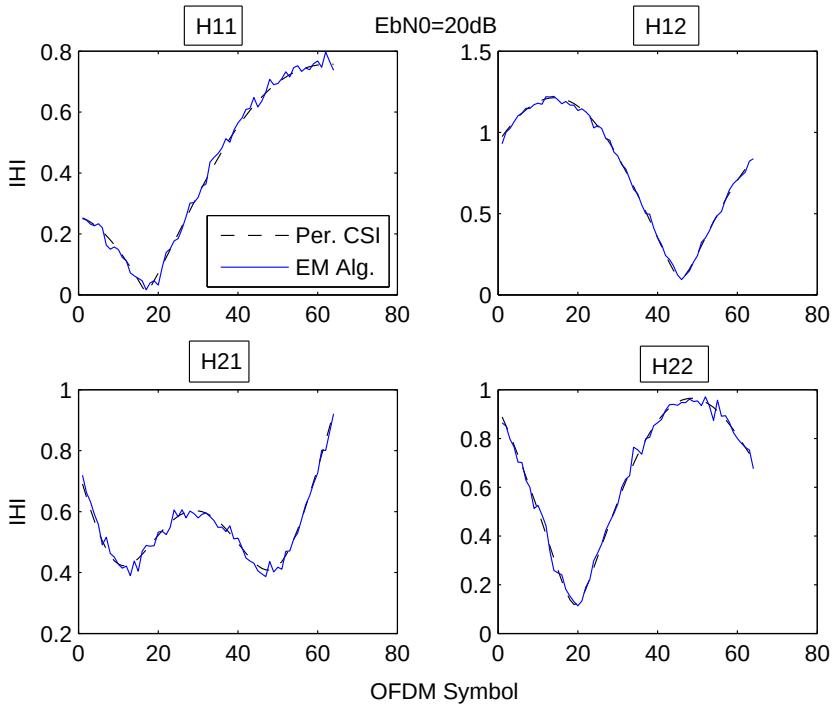

Figure 4.20. Tracking the channel variations of Method 2 in time for V-BLAST OFDM

is used for this simulation too. We can see the BER performance in Figure 4.21. There is a small difference between joint channel estimation and initial estimation.

Figure 4.22 shows the channel estimation performance of these systems. It is seen that by updating the weaker channels the channel estimation performance is improved. Joint channel estimation technique especially gives good results in high SNR region.

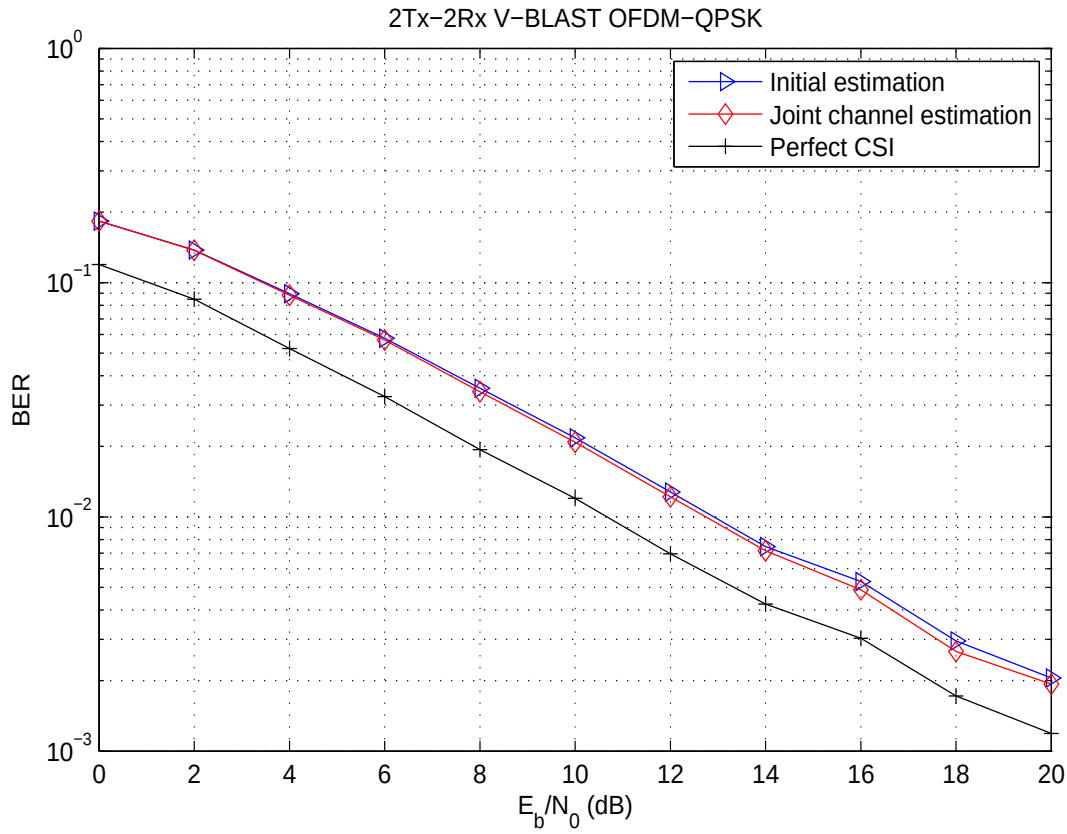

Figure 4.21. V-BLAST OFDM BER performance for joint channel estimation

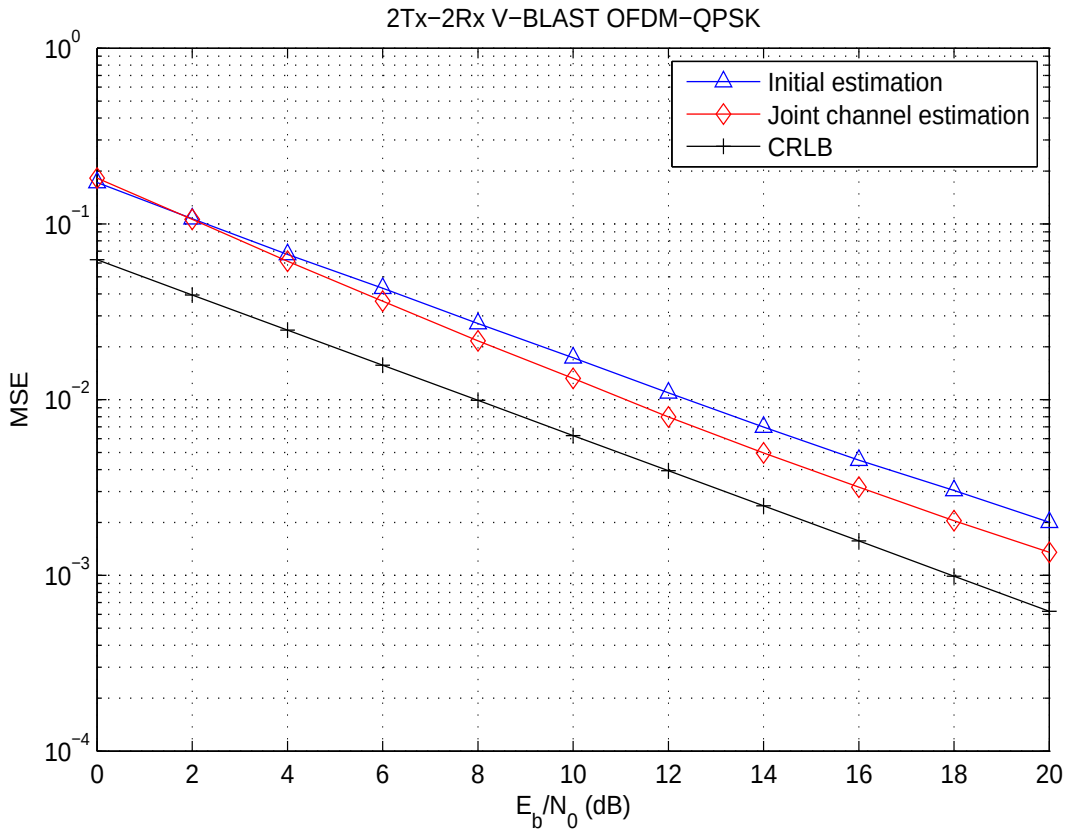

Figure 4.22. V-BLAST OFDM MSE performance for joint channel estimation

CHAPTER 5

CONCLUSION

In this thesis, we have focused on channel estimation techniques for SISO-OFDM and MIMO-OFDM systems. We have aimed to design spectrally efficient and lower complexity system to improve the channel estimation performance.

We have studied pilot-based and Expectation-Maximization (EM)-based channel estimation techniques and have compared their performances in terms of BER, MSE and iteration numbers used in the EM algorithm. We have shown that the EM-based channel estimation algorithm has better performance compared to pilot-based channel estimation for SISO-OFDM systems. We have also compared these algorithms for STBC-OFDM and V-BLAST structured OFDM and have shown that the EM algorithm either improve the channel estimation performance or increase the bit error rate performance.

We have studied two different methods which have different number of pilot symbols and different pilot arrangement in time-frequency axes. We have utilized the EM algorithm to increase channel estimation performance for both methods. We have proposed a lower complexity and spectrally efficient pilot arrangement and compared it with existing pilot arrangement method. We have also used these methods for STBC-OFDM and V-BLAST OFDM. We have shown that the method which has lower number of pilots has the same performance for high SNR values. We have concluded that, the proposed technique is suitable to use for high SNR values in SISO-OFDM, STBC-OFDM and V-BLAST OFDM systems, since it is spectrally efficient and has lower computational complexity.

We have proposed an iterative channel estimation technique, which establishes a link between decision block and channel estimation block, with lower complexity. We have compared this technique with the EM-based channel estimation technique and shown that they have the same performance.

Finally, we have studied joint channel estimation and signal detection technique for V-BLAST-OFDM systems. We have updated the worst estimated channels using the EM algorithm and we have improved the channel estimation performance. Thus, we have increased the BER performance of the system slightly.

As a future work, these iterative channel estimation techniques for SISO-OFDM and MIMO-OFDM will be extended to multiuser communication systems.

REFERENCES

Agrawal, D., Tarokh, V., Naguib, A., and Seshadri, N. 1998. ”Space-time coded OFDM for high data-rate wireless communication over wideband channels.”, Proceedings of IEEE VTC-Spring, Vol. 3, pp. 2232-2236.

Alamouti, S. M. 1998. “A simple transmit diversity technique for wireless communications”, *IEEE Journal on Select Areas in Communications*. Vol. 16, No. 08 pp. 1451-1458.

Barhumi, L., Leus, G., and Moonen, M. 2003. ”Optimal training design for MIMO-OFDM systems in mobile wireless channels.”, *EURASIP Journal on Applied Signal Processing*. Vol. 51, pp. 1615-1624.

Baştürk, İ., Özbek, B. 2007. ”Performance of Pilot-Based EM Channel Estimation for OFDM Systems ”, IEEE Signal Processing and Communications Applications Conference , Eskişehir.

Bello, P. A. 1963. ”Characterization of randomly time-varying linear channels”, *IEEE Transactions on Communications*. Vol. 11, pp. 360-393.

Cimini, L. 1985. “Analysis and simulation of a digital mobile channel using orthogonal frequency multiplexing ”, *IEEE Transactions on Communication*. Vol. 33, No. 07, pp. 665-675.

Clarke, R. H. 1968. ”A statistical theory of mobile-radio reception”, *Bell System Technical Journal*. Vol. 47, pp.957-1000.

Coleri, S., Ergen, M., Puri, A. and Bahai, A. 2002. ”Channel estimation techniques based on pilot arrangement in OFDM systems”, *IEEE Transactions on Broadcasting*. Vol. 48, No. 03, pp. 223-229.

Dempster, A. P., Laird, N. M. and Rubin, D. B. 1977. ”Maximum likelihood from incomplete data via the EM algorithm”, *J. Royal Statiscal Soc., Ser. R.*. Vol. 39, No. 1, pp. 1-38.

Guo, J., Wang, D.and Ran, C. 2003. ”Simple channel estimator for STBC-based OFDM systems”, Electronics letters, Vol. 39 pp. 445-447.

ETSI 1998 ”Channel models for Hiperlan/2 in different indoor scenarios.”, *European Telecommunications Standards Institute*. Norme ETSI, doc.3ERI085B.

ETSI 1999 ”Broadband radio access networks BRAN:Hiperlan type 2 technical specifications part 1-physical layer.”, *ETSI DTS/BRAN030003-1*.

Foschini, G. J. 1996. ”Layered space-time architecture for wireless communications in a fading environment when using multiple antennas ”, *Bell Laboratories Technical Journal*. Vol. 1, No. 2, pp. 41-59.

IEEE 802.11a 1999 ”Part11: Wireless LAN medium access control (MAC) and physical layer (PHY) specifications: High speed PHY in the 5Ghz band.”, *IEEE Std 802.11a-1999.* pp.1-83

IEEE802.16a 2001 ”OFDM mode for the IEEE 802.16a PHY draft standard.”, *MBWA Working Group IEEE 802.16.3c-01/59*.

Jakes, W. C. 1974 ”Microwave mobile communications”, *Wiley-Interscience*.

Lee K. F. and Williams D. B. 2000. ”A space-time coded transmitter diversity technique for frequency selective fading channels.”, Proceedings of Sensor Array and Multichannel Signal Processing Workshop, pp. 149-152.

Lee K. F. and Williams D. B. 2001. ”A multirate pilot-symbol-assisted channel estimator for OFDM transmitter diversity systems.”, Proceedings of IEEE ICASSP, Salt Lake City, UT, USA, Vol. 4 pp. 2409-2412.

Lee K. F. and Williams D. B. 2002. ”Pilot-Symbol Assisted Channel Estimation for Space-Time Coded OFDM Sytems”, *EURASIP Journal on Applied Signal Processing*. Vol. 5, pp. 507-516.

Lu, B., and Wang, X. 2000. ”Space-time code desing in OFDM systems”, Proceedings of IEEE GLOBECOM, Vol. 2 pp. 1000-1004.

Ma, X., Kobayashi H., and Schwartz S. C. 2004. ”EM-Based Channel Estimation Algorithms for OFDM”, *EURASIP Journal on Applied Signal Processing*. Vol. 10, pp. 1460-1477.

Moon, T. K . 1996. ”The Expectation-Maximization Algorithm”, *IEEE Signal Processing Magazine*. pp. 47-60.

Özbek B., Ruyet D. L., and Panazio C. 2005. ”Pilot-Symbol Aided Iterative Channel Estimation for OFDM-Based Systems”, Proceedings of EUSIPCO 2005, Antalya.

Rappaport, T. S, 1996. *Wireless Communications: Principles and practise*, (Prentice Hall, New Jersey, 1996). pp. 139-196

Song, B., Zhang, W., Gui, L. 2005. ” EM based joint channel estimation and signal detection for V-BLAST in MIMO OFDM systems.”, Proceedings of Wireless Communications, Networking and Mobile Computing, Vol. 1, pp. 135-138

Tarokh, V., Seshadri, N. and Calderban, A. R. 1998. ”Space-time codes for high data rate wireless communication: Performance criterion and code construction”, *IEEE Transaction on Information Theory*. Vol. 44, No. 2, pp. 744-765.

Van de Beek, J. J., Edfors, O. S., Sandell, M., Wilson, S. K., and Börjesson, O. P. 1995. ”On channel estimation in OFDM systems.”, Proceedings of IEEE Vehicular Technology Conference (VTC 95), Chicago, Vol. 2, pp. 815-819.

Wolniansky, P. W., Foschini, G. J., Golden, G. D. and Valenzuela, R. A. 1998. ”V-BLAST : An architecture for realizing very high data rates over the rich-scattering wireless channel ”, Proceedings of URSI International Symposium on Signals, Systems, and Electronics, pp. 295-300.